Journal of Computational Physics **181,** 222–259 (2002)
doi:10.1006/jcph.2002.7122

A Coupled Schrödinger Drift-Diffusion Model for Quantum Semiconductor Device Simulations

P. Degond* and A. El Ayyadi†

**MIP, UMR 5640 (CNRS-UPS-INSA), Université Paul Sabatier, 118, Route de Narbonne, 31062 Toulouse Cedex, France; and †MIP, UMR 5640 (CNRS-UPS-INSA), INSA, 135, Avenue de Rangueil, 31077 Toulouse Cedex, France*

E-mail: degond@mip.ups-tlse.fr, Asma.ElAyyadi@gmm.insa-tlse.fr

Received November 21, 2001; revised May 31, 2002

In this paper, we derive a coupled Schrödinger drift–diffusion self-consistent stationary model for quantum semiconductor device simulations. The device is decomposed into a quantum zone (where quantum effects are expected to be large) and a classical zone (where they are supposed negligible). The Schrödinger equation is solved for scattering states in the quantum zone while a drift–diffusion model is used in the classical zone. The two models are coupled through interface conditions which are derived from those of N. Ben Abdallah (1998, *J. Stat. Phys.* **90**, 627) through a diffusion approximation. Numerical tests in the case of a resonant tunneling diode illustrate the validity of the method. © 2002 Elsevier Science (USA)

Key Words: Boltzmann equation; Schrödinger equation; quantum–classical coupling; scattering states; diffusion approximation; Milne problem.

1. INTRODUCTION

In this work, we present a hybrid classical–quantum stationary model for electron transport in one-dimensional semiconductor devices. We are aiming at devices which exhibit a well-localized quantum region, while the rest of the device behaves classically. Examples of such devices are the resonant tunneling diodes.

Resonant tunneling diodes are such that a narrow potential well is flanked by two potential barriers, themselves imbedded in the low-doped region of a unipolar diode. These structures exhibit a resonant quantum state inside the barrier. By tuning the applied bias, it is possible to line up the Fermi level (which represents the typical energy of the electrons in the source contact) with the resonant energy. In such a configuration, quantum tunneling increases the transmission current, as opposed to configurations where the Fermi energy and the resonant

0021-9991/02 $35.00

state are off-line. Therefore, this kind of device exhibits nonmonotonous current-voltage characteristics, which are of great interest for logic applications.

In a resonant tunneling diode, it is expected that quantum effects are localized in the vicinity of the double barriers, while transport in the access zones (the highly doped regions connected with the contacts) and the area downstream from the double-barrier is mainly classical. Therefore, it seems attractive to develop a hybrid model which provides a complete quantum description of the physics wherever necessary but degenerates to a semiclassical model when quantum effects are negligible. The aim of the present work is to describe such a coupling methodology.

The fact is that quantum transport simulations are complex and computationally expensive. They require the self-consistent resolution of a quantum transport model with the Poisson equation. Much effort has been devoted to the Wigner equation (see the review in [22] and references therein, and also [27, 31]). Simplified models make use of a semiclassical approximation of the charge density [33].

It is not an easy matter to incorporate particle scattering in quantum transport simulations. Many theoretical approaches have been proposed (see, e.g., [1, 10, 19, 30, 37]). Yet no agreement on the model has been reached to date. Stationary scattering models have successfully predicted the collision-dominated regime [13, 20, 43] but cannot handle the collisionless regime. A related approach is based on the Pauli master equation (see, e.g., [21, 28]) but requires negligible quantum correlations, which is sometimes questionable. Some authors simply use the semiclassical electron–phonon collision term in the Wigner equation [22, 31], even though the Wigner function is not always positive. The full quantum treatment of electron–phonon interaction is very computationally demanding [26]. Quantum hydrodynamics and quantum drift–diffusion models have been investigated (e.g., in [12] and [34], respectively), but information is lacking about what an equation-of-state for quantum electron gases should be.

Semiclassical models are computationally far less expensive than quantum ones and have been practiced for years now (see, e.g., [38] and references therein). Using a hybrid classical–quantum approach allows us to shrink the size of the quantum system to be simulated and therefore reduces the overall cost of the simulation. Furthermore, collisions are easily included in semiclassical models [38]. If the quantum region is small enough, using a collisionless model in this region may be an acceptable approximation, which is justified as long as the electron transit time does not exceed the mean collision time. This is usually the case in many practical situations. Therefore, it is often accurate enough to use a collisional model in the classical region and a collisionless model in the quantum region. This is the option we take in the present work. Note that similar hybrid approaches have already been proposed in the literature (see, e.g., [32], and more recently [4, 9]). Our approach differs from these in the choice of either the models or the coupling methodology.

In the present work, we use a drift–diffusion model in the classical zone. Such models can be derived from semiclassical kinetic models under the assumption of small mean free path and are valid when collisions dominate over all other transport effects. Therefore, our model in the classical zone is a highly collisional one.

This derivation is based on the diffusion approximation method, which has been widely used in various physical contexts (see, e.g., [3, 8, 29] in the context of neutron transport, [2] for radiative transfer, [5, 25, 35] for semiconductors, and [16] for plasmas). This approach also allows us to derive adequate boundary conditions (i.e., taking into account the kinetic boundary layer; see, e.g., [3, 16]) or interface conditions (see, e.g., [17] for semiconductor

heterojunctions). We rely on this procedure to derive our coupling conditions between the classical and quantum regions.

Our starting point is a hybrid kinetic–quantum model derived by Ben Abdallah [4]. In this model, the scattering states and amplitudes of the quantum region are obtained from the Schrödinger equation, while, in the classical region, the Boltzmann transport equation is solved for the semiclassical distribution function. At the classical–quantum interface, the distribution function satisfies reflection–transmission conditions depending on the quantum scattering amplitudes and is used as an "alimentation function" to construct the quantum density matrix and charge concentration. The potential is linked to the classical and quantum charge concentrations by the Poisson equation. This coupling model is current-preserving through the classical–quantum interface, which is an important check of its physical consistency.

In the present paper, we proceed to a diffusion approximation of Ben Abdallah's [4] model and replace the Boltzmann equation *together with its reflection–transmission conditions* at the interface by a drift–diffusion model *with adequate connection conditions*. The key point and novelty of the present work is in the derivation of these connection conditions. For that purpose, we use kinetic boundary layer analysis, according to [3] and [17]. The rest of Ben Abdallah's [4] model (mainly the treatment of the quantum region and the Poisson equation) is left unchanged.

In our one-dimensional model, we consider a device occupying the interval $[0, L]$, in which the quantum zone $Q = [x_1, x_2]$ (with $0 < x_1 < x_2 < L$) is sandwiched between two classical zones $C = [0, x_1] \cup [x_2, L]$. The coupling of the drift–diffusion model in the C zone with the quantum model in the Q zone is realized through connection conditions relating the drift–diffusion unknowns (namely the electron density n and the current density j) at the two interface points x_1 and x_2. These conditions are

$$j(x_1) = j(x_2) := j, \tag{1.1}$$

$$n(x_1)e^{-V(x_1)/U_{th}} - n(x_2)e^{-V(x_2)/U_{th}} = \theta_Q j, \tag{1.2}$$

where θ_Q is a constant which depends on the scattering amplitudes of the quantum potential. In the above relation, $U_{th} = k_B T/e$ is the thermal potential (k_B being the Boltzmann constant, T the lattice temperature, and e the elementary (positive) charge). Relation (1.2) can be equivalently written as a jump relation for the quasi Fermi levels $\varphi_n = U_{th} \ln n - V$:

$$e^{\varphi_n(x_1)/U_{th}} - e^{\varphi_n(x_2)/U_{th}} = \theta_Q j. \tag{1.3}$$

That the current conservation relation (1.1) should hold is physically obvious. Similarly, at equilibrium (when $j = 0$), (1.3) imposes the continuity of the Fermi level, as it should. However, away from equilibrium, (1.3) states that the jump of the (exponential of the) Fermi levels should be proportional to the current through the structure. The proportionality coefficient θ_Q is where the quantum scattering amplitudes enter, and it must therefore be accurately determined and computed. The core of the present paper is to discuss this point. Then, as in [4], the classical density at the interface determines a charge concentration in the quantum region. This, together with its counterpart in the classical region, is used in the Poisson equation for the computation of the self-consistent potential.

The paper is organized as follows. The overall model is introduced in Section 2, without details about its derivation. The numerical method and results are displayed and discussed

in Section 3, and a conclusion follows in Section 4. Sections 5 to 8 are appendices which provide more details about the derivation of the model: Section 5 recalls the main steps of the passage from the Boltzmann equation to the drift–diffusion model. In Section 6, we derive the transmission condition from the layer analysis of the kinetic model. Sections 7 and 8 provide two methods for calculating the coefficient θ_Q which appears in the transmission condition.

2. PRESENTATION OF THE METHOD

2.1. The Quantum Region

We consider a device occupying the interval $\Omega = [0, L]$, in which the quantum zone $Q = [x_1, x_2]$ (with $0 < x_1 < x_2 < L$) is sandwiched between two classical zones $C = [0, x_1] \cup [x_2, L]$. Let us first assume that the electric potential $V(x)$ is given and known throughout the structure Ω and let us concentrate on the quantum model in the Q region. For that purpose, we define a potential $\tilde{V}$ which coincides with the potential V inside the quantum zone Q and is extended by continuity into constant functions outside Q:

$$\tilde{V}(x) = \begin{cases} V_1 := V(x_1) & x \le x_1 \\ V(x) & x_1 \le x \le x_2 \\ V_2 := V(x_2) & x \ge x_2. \end{cases} \tag{2.1}$$

From now on, we shall suppose that $V_2 > V_1$ to fix the ideas and note $\delta V = V_2 - V_1$. The effective mass $m(x)$ is allowed to be position dependent in the quantum zone Q but is constant in C and has the same value in $[0, x_1]$ and $[x_2, L]$. We denote this common value by m.

As a quantum model for the Q region, we actually consider the Schrödinger equation over the full real line $\mathbb{R}$ in the potential $\tilde{V}$. More precisely, we introduce the scattering states ψ_p, $p \in \mathbb{R}$, solutions of

$$\frac{-\hbar^2}{2} \frac{d}{dx}\left(\frac{1}{m(x)} \frac{d\psi_p}{dx}(x)\right) - e\tilde{V}(x)\psi_p = (E_p - eV_b)\psi_p, \tag{2.2}$$

where $\hbar$ is the reduced Planck constant. In particular, $p > 0$ stands for the right-going scattering states, while $p < 0$ points at the left-going scattering states. V_b is the value of the potential at the upstream boundary of Q, namely,

$$V_b = V(x_1) \quad \text{for } p > 0, \quad V_b = V(x_2) \quad \text{for } p < 0,$$

while E_p is the energy of the corresponding state measured with origin of energies at V_b:

$$E_p = \frac{p^2}{2m}.$$

Consequently, measured relative to the absolute origin of energies, $E_p - eV_b$ is the total energy of the corresponding scattering state.

The scattering states are uniquely defined as solutions of (2.2) together with the following conditions for $p > 0$:

$$\psi_p(x) = \exp\frac{ip(x - x_1)}{\hbar} + r(p)\ \exp\frac{-ip(x - x_1)}{\hbar}, \quad x < x_1, \tag{2.3}$$

$$\psi_p(x) = t(p) \exp\left(\frac{i}{\hbar} p_+(p)(x - x_2)\right), \quad x > x_2. \tag{2.4}$$

And for $p < 0$:

$$\psi_p(x) = \exp\frac{-ip\,(x - x_2)}{\hbar} + r(p) \exp\frac{ip(x - x_2)}{\hbar}, \quad x > x_2, \tag{2.5}$$

$$\psi_p(x) = t(p) \exp\left(-\frac{i}{\hbar} p_-(p)(x - x_1)\right), \quad x < x_1, \tag{2.6}$$

where

$$p_+(p) = (p^2 + 2em\,\delta V)^{1/2}, \quad p_-(p) = (p^2 - 2em\,\delta V)^{1/2}.$$

Note that for $-p_\delta \le p \le 0$ with $p_\delta = \sqrt{2em\delta V}$, $p_-(p)$ is a pure imaginary number. The coefficients $r(p)$ and $t(p)$ are, respectively, the reflection and transmission amplitudes. They are explicitely given in terms of the solution by:

$$r(p) = \frac{1}{2}\left(\psi_p + \frac{i\hbar}{p}\frac{\partial \psi_p}{\partial x}\right)(x_1), \quad t(p) = \psi_p(x_2), \quad \text{for } p > 0,$$

$$r(p) = \frac{1}{2}\left(\psi_p - \frac{i\hbar}{p}\frac{\partial \psi_p}{\partial x}\right)(x_2), \quad t(p) = \psi_p(x_1), \quad \text{for } p < 0.$$

It should also be noticed that finding the scattering states is equivalent to finding solutions of the Schrödinger equation (2.2) on the bounded interval $[x_1, x_2]$ with the following boundary conditions (as the convenient combination of Eqs. (2.3), (2.4) (for the right-going states) and (2.5), (2.6) (for the left-goings states) would show). For $p > 0$:

$$\psi_p'(x_1) = \frac{2ip}{\hbar} - \frac{ip}{\hbar}\psi_p(x_1), \quad \psi_p'(x_2) = \frac{i}{\hbar} p_+(p)\psi_p(x_2). \tag{2.7}$$

For $p < 0$:

$$\psi_p'(x_1) = -\frac{i}{\hbar} p_-(p)\,\psi_p(x_1), \quad \psi_p'(x_2) = -\frac{2ip}{\hbar} + \frac{ip}{\hbar}\psi_p(x_2). \tag{2.8}$$

The reflection and transmission coefficients $R(p)$ and $T(p)$ are defined by:

$$R(p) = |r(p)|^2, \quad T(p) = p_\pm(p)|t(p)|^2/p, \quad \pm p > 0.$$

We recall that

$$T(p) + R(p) = 1, \quad i = 1, 2, \quad p \in \mathbb{R},$$

and that $R(p) = 1$ for $-p_\delta \le p \le 0$. We also recall the reciprocity relation:

$$T(p) = T(-p_+(p)), \quad \forall p > 0, \quad T(p) = T(p_-(p)), \quad \forall p < -p_\delta. \tag{2.9}$$

We finally note that $p_+(p_-(p)) = p_-(p_+(p)) = p$, whenever the terms are defined.

Let us temporarily assume that the distribution function $f(x, p)$ (where $x \in C$ is the position and $p \in \mathbb{R}$ is the momentum) in the classical zone $C = [0, x_1] \cup [x_2, L]$ is known. Its values $f(x_1, p)$ for $p > 0$ and $f(x_2, p)$ for $p < 0$ correspond to particles entering the quantum region Q. Following [4], we use these values as an "alimentation function," to construct a quantum density matrix in Q,

$$\rho_Q(x, x') = N^{-1}\bigg(\int_{p>0} f(x_1, p)\psi_p(x)\overline{\psi_p(x')}\, dp + \int_{p<0} f(x_2, p)\psi_p(x)\overline{\psi_p(x')}\, dp \bigg), \quad x, x' \in Q, \tag{2.10}$$

as well as the electron density $n(x)$:

$$n(x) = \int_{p>0} f(x_1, p)|\psi_p(x)|^2\, dp + \int_{p<0} f(x_2, p)|\psi_p(x)|^2\, dp, \quad x \in Q. \tag{2.11}$$

The number N is the total number of particles in the Q region,

$$N = \int_{x_1}^{x_2} n(x)\, dx,$$

so that the density matrix ρ_Q is of unit trace. From ρ_Q, all physical observables can be computed, such as the particle current:

$$j = \hbar\bigg(\int_{p>0} f(x_1, p)\Im m\bigg(\frac{1}{m(x)} \frac{\partial \psi_p}{\partial x}(x)\overline{\psi_p(x)} \bigg) dp + \int_{p<0} f(x_2, p)\Im m\bigg(\frac{1}{m(x)} \frac{\partial \psi_p}{\partial x}(x)\overline{\psi_p(x)} \bigg) dp \bigg), \quad x \in Q. \tag{2.12}$$

We now turn to the description of the model in the classical region.

2.2. The Classical Region

As we noted above, the classical region is disconnected. In the open intervals $C_1 = (0, x_1)$ and $C_2 = (x_2, L)$, we solve the stationary drift–diffusion model

$$\frac{dj}{dx} = 0, \tag{2.13}$$

$$j = -D(x)\bigg(\frac{dn}{dx} - n\frac{d}{dx}\bigg(\frac{V}{U_{th}} \bigg) \bigg), \tag{2.14}$$

where $n(x)$, $j(x)$ now denote the electron number and momentum densities in the classical region, $U_{th} = k_B T_L/e$ is the thermal potential (k_B being the Boltzmann constant, T_L the lattice temperature, and e the elementary positive charge), and $D(x)$ is the diffusivity. We

note that according to Einstein's relation, the mobility is supposed equal to D/U_{th}. We assume that the temperature T_L is uniform over the structure.

The two open sets C_i are connected each one with each other through the conditions

$$j(x_1) = j(x_2) := j, \tag{2.15}$$

$$n(x_1)e^{-V(x_1)/U_{th}} - n(x_2)e^{-V(x_2)/U_{th}} = \theta_Q j, \tag{2.16}$$

where the number $\theta_Q > 0$ depends on the reflection–transmission coefficients $R(p)$ and $T(p)$ of the quantum region. We describe this relation in detail below. For the time being, we complete the description of the coupling of the classical and quantum regions.

First, we supplement the problem with Dirichlet boundary conditions at $x = 0$ and $x = L$,

$$n(0) = n_D(0), \quad n(L) = n_D(L), \tag{2.17}$$

where $n_D(x)$, $x \in [0, L]$ is the doping concentration, i.e., the concentration of positively ionized impurities. It is easy to show that Eqs. (2.13) and (2.14), together with transmission conditions (2.15) and (2.16) and boundary condition (2.17), are well-posed, i.e., they have a unique solution, as soon as θ_Q is nonnegative. From the density, we construct a distribution function in the C region by assuming that the momentum dependence is Maxwellian;

$$f(x, p) = n(x)M(p), \quad M(p) = \frac{1}{\sqrt{2\pi}\, p_{th}} \exp - \frac{p^2}{2p_{th}^2}, \quad x \in C, \quad p \in \mathbb{R}, \tag{2.18}$$

where $p_{th} = \sqrt{mk_B T_L}$ is the thermal momentum. This is the distribution function to be used as an alimentation function in formulae (2.10)–(2.12) for the quantum region.

Finally, the potential $V(x)$ is a solution of the Poisson equation

$$-\frac{dV}{dx}\left(\epsilon(x)\frac{dV}{dx}\right) = e(n_D(x) - n(x)), \quad x \in \Omega, \tag{2.19}$$

with the boundary conditions

$$V(0) = 0, \quad V(L) = V_L, \tag{2.20}$$

where $V_L > 0$ is the total applied bias, and $\epsilon(x)$ is the material permittivity. In (2.19), the density $n(x)$ is equal to the classical density (solution of the drift–diffusion problem (2.13), (2.14)) in C and to the quantum density (2.14) in Q.

A solution algorithm for the problem is the following. First, let a first guess of the potential V be given. We compute the scattering states ψ_p and the reflection-coefficients $R(p)$, $T(p)$ of the quantum region Q in the potential $\tilde{V}$. Then, a value of the coupling constant θ_Q is deduced, which allows us to solve the drift–diffusion problem with the transmission conditions (2.16). An alimentation function is deduced from (2.18), which, together with the scattering states, allows us to construct a quantum density according to (2.11). Then, the Poisson equation can be solved for an updated value of the potential and the iteration can be continued. We shall see that this is not the most efficient way to conduct the iterations. However, this simple picture gives an intuitive idea of how the various parts of the model are related.

2.3. The Extrapolation Coefficient θ_Q

We now describe how θ_Q is obtained. We note that it has the physical dimension of the inverse of a velocity. It is sometimes called the extrapolation coefficient [3]. To define θ_Q, we must go back to the kinetic description of the classical zone, as proposed by Ben Abdallah [4].

2.3.1. *From Kinetic to Drift–Diffusion Models*

In the model of [4], the distribution function $f(x, p)$, $x \in C$, $p \in \mathbb{R}$ solves a Boltzmann equation,

$$\frac{p}{m}\frac{\partial f}{\partial x} + e\frac{dV}{dx}\frac{\partial f}{\partial p} = Q(f), \quad x \in C, \quad p \in \mathbb{R}, \tag{2.21}$$

where $Q(f)$ is the collision operator. We consider a very simplified model for the lattice defects collision operator and we neglect electron–electron collisions as well as degeneracy effects. This operator is written [35]

$$Q(f)(p) = \int_{\mathbb{R}} S(x, p, p')(M(p)f(p') - M(p')f(p))\,dp', \tag{2.22}$$

where M is the Maxwellian given by (2.18). Note that $\int M(p)\,dp = 1$. The function S is related to the collision transition rate and is supposed symmetric and positive: $S(x, p, p') = S(x, p', p)$, $S \geq 0$. In many practical applications, it is supposed constant with respect to p and p';

$$S(x, p, p') = \tau(x)^{-1}, \tag{2.23}$$

where $\tau(x)$ is the mean time between collisions, possibly depending on x through the material properties. In this case, the diffusivity of the drift–diffusion model is given by

$$D(x) = \tau v_{th}^2, \quad v_{th} = \sqrt{\frac{k_B T_L}{m}}, \tag{2.24}$$

where v_{th} is the thermal velocity.

For a general transition rate S, the formula for the diffusivity is more involved. We first recall that Q, on a convenient function space, is a self-adjoint operator with null space of dimension one, spanned by the Maxwellians. Its range is characterized by functions with zero momentum average. Therefore, for a given function g, the equation

$$Q(f) = g \tag{2.25}$$

is uniquely solvable in f provided that g satisfies $\int g(p)\,dp = 0$ and that f is searched for among functions such that $\int f(p)\,dp = 0$. By abuse of notation, we denote by $f = Q^{-1}(g)$ this unique solution. Now, we let

$$h = -Q^{-1}\left(\frac{p}{m}M(p)\right), \tag{2.26}$$

which is well defined since the function pM is odd. The diffusivity is given in terms of h by

$$D(x) = \int_{p\in\mathbb{R}} \frac{p}{m} h(p)\, dp \tag{2.27}$$

and depends on x since Q, and therefore h, may depend on it. All the above statements are made precise in Section 5.

The first two terms of the expansion of f in powers of the scaled mean free path α (α being defined as the ratio of the collision mean free path to the characteristic length of the device, see Section 5) are given by

$$f = f^0 + \alpha f^1 + O(\alpha^2), \quad f^0 = n(x,t)M(p), \quad f^1 = \ell(p) j, \tag{2.28}$$

with

$$\ell(p) = \frac{h(p)}{D}, \tag{2.29}$$

n being the solution of the drift–diffusion equation. The function ℓ measures the first-order response of the system to deviations from global equilibrium, which occurs when gradients of n or V are present.

2.3.2. *The Transmission Conditions through the Quantum Zone at the Kinetic Level*

In [4], the kinetic model (2.21) is coupled with the quantum model described in Section 2.1 through the following interface conditions relating the values of the distribution function at x_1 and x_2:

$$f(x_1, p) = R(-p) f(x_1, -p) + T(-p_+(p)) f(x_2, -p_+(p)), \quad p < 0, \tag{2.30}$$

$$f(x_2, p) = R(-p) f(x_2, -p) + T(p_-(p)) f(x_1, p_-(p)), \quad p > p_\delta, \tag{2.31}$$

$$f(x_2, p) = f(x_2, -p), \quad 0 < p < p_\delta. \tag{2.32}$$

Conditions (2.30)–(2.32) find an easy interpretation. Consider for instance (2.30). It states that particles entering C at x_1 (which contribute to building up $f(x_1, p)$ for $p < 0$) are either particles which have exited C at x_1 with momentum $-p$ and have undergone a reflection by Q (with probability $R(-p)$), or particles which have exited C at x_2 with momentum $-p_+(p)$ and have been transmitted through Q (with probability $T(-p_+(p))$). A similar interpretation is valid for $f(x_2, p)$ for $p > p_\delta$, leading to (2.31). For $0 < p < p_\delta$, there is no particle transmitted from x_1 (note that $p_-(p)$ is a pure imaginary number), so that only reflection occurs, leading to (2.32). In view of the reciprocity condition (2.9), we can rewrite (2.30)–(2.32) according to

$$\mathcal{B}(f_1, f_2) = 0, \tag{2.33}$$

where $f_i(p) := f(x_i, p)$ and the linear operator $\mathcal{B}$ is defined by:

$$\mathcal{B}(f_1, f_2)(p) = \begin{cases} f_1(p) - (R(-p) f_1(-p) + T(-p) f_2(-p_+(p))), & p < 0, \\ f_2(p) - (R(-p) f_2(-p) + T(-p) f_1(p_-(p))), & p > p_\delta, \\ f_2(p) - f_2(-p), & 0 < p < p_\delta. \end{cases} \tag{2.34}$$

The particle flux for the kinetic model is given by:

$$j(x) = \int_{\mathbb{R}} f(x, p)\frac{p}{m}\, dp. \tag{2.35}$$

It is proved in [4] that the transmission condition (2.33) is current-preserving, i.e.,

$$j_K(x_1) = j_K(x_2). \tag{2.36}$$

Moreover, the kinetic and quantum fluxes coincide at the interface. Namely,

$$j_K(x_1) = j_Q(x_1), \quad j_K(x_2) = j_Q(x_2),$$

where j_Q is given by (2.12).

Another noticeable property of the operator $\mathcal{B}$ is that two Maxwellians $f_i = n_i M(p)$ satisfy the transmission condition (2.33) if and only if the n_i's are linked through

$$n_1 e^{-V_1/U_{th}} - n_2 e^{-V_2/U_{th}} = 0. \tag{2.37}$$

2.3.3. *Definition of the Extrapolation Constant θ_Q*

To proceed in the definition of θ_Q, we need to introduce an auxiliary problem (often referred to as a Milne problem [3]). First, define $\ell_i(p) = \ell(x_i, p)$, $i = 1, 2$, with ℓ given by (2.29). We search for two functions $\theta_1(x, p)$ and $\theta_2(x, p)$ respectively defined for $(x, p) \in (-\infty, 0] \times \mathbb{R}$ and $[0, \infty) \times \mathbb{R}$, solutions of the problem

$$\frac{p}{m}\frac{\partial \theta_i}{\partial x} = Q_i(\theta_i), \quad p \in \mathbb{R}, \quad x \in \Theta_i, \tag{2.38}$$

where $\Theta_1 = (-\infty, 0)$ and $\Theta_2 = (0, \infty)$, and satisfying

$$\mathcal{B}(\theta_1(0, p) - \ell_1(p), \theta_2(0, p) - \ell_2(p)) = 0. \tag{2.39}$$

In Section 6, it is shown that problem (2.38), (2.39) has a solution (θ_1, θ_2), such that $\theta_i M^{-1}$ is bounded on Θ_i. Moreover, this solution is unique up to the addition of a Maxwellian. More precisely, if (θ_1, θ_2) and (θ_1', θ_2') are two solutions, then there exist two real numbers n_1, n_2 related by relation (2.37) such that

$$(\theta_2' - \theta_2)(x, p) = n_2 M, \quad \forall x \in \Theta_2, \quad (\theta_1' - \theta_1)(x, p) = n_1 M, \quad \forall x \in \Theta_1.$$

Furthermore, $\theta_i(x, p)$ converges towards a Maxwellian when $|x|$ tends to infinity, with exponential rate. Let $n_{\theta_i}^{\infty}$ be the density associated with this Maxwellian; i.e.,

$$\theta_i(x, p) \to n_{\theta_i}^{\infty} M_i \quad \text{when } |x| \to \infty, \quad x \in \Theta_i.$$

Then, the real number

$$\theta_Q = e^{-V_2/U_{th}} n_{\theta_2}^{\infty} - e^{-V_1/U_{th}} n_{\theta_1}^{\infty}, \tag{2.40}$$

does not depend on the chosen solution. This is the number to be used in (2.16).

To understand this construction, it should be noted that the leading order term f^0 of the Hilbert expansion (2.28), being Maxwellian, exactly satisfies the kinetic transmission condition (2.33) as soon as the densities are related by (2.37). However, this is not the case of the first-order corrections f^1 in the expansion (2.28), because ℓ is not a Maxwellian. This means that a layer corrector must be defined. This layer term is defined in terms of the functions θ_i. The transmission condition then applies to the asymptotic limits θ_i, which explains the occurrence of the number θ_Q.

2.4. Approximate Analytical Formulae for θ_Q

In general, there exist no exact analytical formulae for θ_Q. However, for the numerical efficiency of the whole procedure, it is important to find approximate analytical formulae. Indeed, a complete numerical integration of problem (2.38), (2.39) at each iteration step of the algorithm would be extremely costly. We present two approximate formulaes for θ_Q. The first one is based on an approximation of the albedo operator; the second one is based on an iterative procedure first proposed by Golse and Klar [24].

2.4.1. *Approximation of the Albedo Operator*

The albedo operator is defined the following way. Let $\chi_0^+(p)$ be a function defined for $p > 0$ and consider the problem of finding a function $\chi(x, p)$ for $(x, p) \in [0, \infty) \times \mathbb{R}$ such that

$$\frac{p}{m}\frac{\partial \chi}{\partial x} = Q(\chi), \quad \chi(0, p) = \chi_0^+(p) \quad \text{for } p > 0. \tag{2.41}$$

In (2.41), the boundary condition only specifies χ for incoming momenta (i.e., corresponding to particles entering the domain $[0, \infty)$), hence the restriction $p > 0$. From [35], there exists a unique solution χ such that $M^{-1}\chi$ is bounded on $[0, \infty) \times \mathbb{R}$. Furthermore, this solution has vanishing flux ($\int \chi(x, p) p\, dp = 0$ for all $x > 0$) and converges to a Maxwellian $\chi_\infty M(p)$ as $x \to \infty$ with an exponential rate. The albedo operator $\mathcal{A}$ maps the known incoming boundary condition χ_0^+ to the unknown outgoing distribution function $\chi(0, p)$ for $p < 0$, which will be denoted by $\chi_0^-(p)$:

$$(\mathcal{A}\chi_0^+)(p) = \chi_0^-(p), \quad p < 0.$$

The albedo operator is a useful tool in the investigation of problem (2.38), (2.39) [17]. Albedo problems have been systematically studied in [11].

In the present section, in order to find an approximation of θ_Q, we suppose that the albedo operator maps any function to a Maxwellian, i.e.,

$$\chi_0^-(p) = n_\chi^- M(p), \quad p < 0,$$

where the constant n_χ^- is related to χ_0^+ by the zero flux condition:

$$n_\chi^- \int_0^\infty Mp\, dp = \int_0^\infty \chi_0^+(p) p\, dp. \tag{2.42}$$

This approximation can be justified by the very fast relaxation of the solution towards a Maxwellian. It is used in a large number of practical applications [23]. If this approximation

is valid, the solutions θ_i of (2.38), (2.39) satisfy

$$\theta_1(0, p) = n_{\theta_1}^- M(p) \quad \text{for } p > 0, \quad \theta_2(0, p) = n_{\theta_2}^- M(p) \quad \text{for } p < 0, \tag{2.43}$$

where θ_i^- are constants related with θ_i through a relation like (2.42).

Using the conservation properties of the Milne problem, it is possible to derive the following formula, later refered to as the "albedo" approximation formula:

$$\begin{aligned}\theta_Q \approx \bar{\theta}_Q^a = 2 \int_0^\infty & \left((\ell_2)^2 e^{-V_2/U_{th}} + (\ell_1)^2 e^{-V_1/U_{th}}\right) \frac{p}{m} \frac{dp}{M} \\ & + e^{-V_1/U_{th}} \left(\int_0^\infty T M \frac{p}{m}\, dp \right)^{-1} \left(1 - \int_0^\infty [\ell_1(p) + \ell_2(p_+(p))] T \frac{p}{m}\, dp \right)^2 \\ & - e^{-V_1/U_{th}} \int_0^\infty [\ell_1(p) + \ell_2(p_+(p))]^2 T \frac{p}{m} \frac{dp}{M}. \end{aligned} \tag{2.44}$$

The proof of formula (2.44) can be found in Appendix C, Section 7. We also show that

$$\bar{\theta}_Q^a > 0. \tag{2.45}$$

In the case of a relaxation time operator ((2.22) with (2.23)), ℓ_i is independent of τ, and thus of i. It is given by

$$\ell_i = \frac{p}{k_B T_L} M. \tag{2.46}$$

The leading contribution to $\bar{\theta}_Q^a$ is the second term, which contains the reciprocal of $\int T M (p/m)\, dp$. Indeed, because the transmission resonance is very sharply peaked, only a very small interval of momenta gives rise to a nonzero contribution to the integral. Therefore, the integral is very small and its reciprocal is large.

2.4.2. *Iterative Procedure of Golse–Klar*

The approximation (2.44) is not an approximation in the usual sense since it cannot be improved in an obvious way by tuning some numerical parameter. The method of Golse–Klar [24] does not have this drawback since it can be viewed as a first step of an iterative procedure which, at least formally, converges to the solution of the Milne problem. However, we stop the iterations after either the first or second steps, as we wish to keep analytically tractable formulas. The method is more easily presented in the case of a constant transition rate (2.23). The iterative method and the computations are presented in detail in Section 8. Here, we only display the result,

$$\theta_Q \approx \bar{\theta}_Q^M = e^{-V_1/U_{th}} \vartheta_1, \tag{2.47}$$

$$\theta_Q \approx \bar{\theta}_Q^{GK} = e^{-V_1/U_{th}} (\vartheta_1 + \vartheta_2), \tag{2.48}$$

$$\vartheta_1 = \left(\int_0^\infty T M \frac{p}{m}\, dp \right)^{-1} \left(1 - \int_0^\infty [\ell_1(p) + \ell_2(p_+(p))] T \frac{p}{m}\, dp \right), \tag{2.49}$$

$$\vartheta_2 = \left(\int_0^\infty TM\frac{p}{m}\,dp\right)^{-1}\Bigg[-\vartheta_1\int_0^\infty TMF_0\frac{p}{m}\,dp - \int_0^\infty T[\ell_1(p)+\ell_2(p_+(p))]F_0\frac{p}{m}\,dp + 2e^{-\delta V/U_{th}}\int_0^{p_\delta}\ell_2\,F_+(p)\frac{p}{m}\,dp + 2\int_0^\infty\left[e^{-\delta V/U_{th}}\ell_2(p_+(p))F_+(p_+(p))+\ell_1(p)F(p)\right]\frac{p}{m}\,dp\Bigg], \tag{2.50}$$

where

$$F(p) = \left(\frac{p^2}{p_{th}^2}-1\right)\int_0^\infty \frac{T(p')M(p')}{p'+p}p'\,dp', \tag{2.51}$$

$$F_+(p) = \left(\frac{p^2}{p_{th}^2}-1\right)\int_0^\infty \frac{T(p')M(p')}{p_+(p')+p}p'\,dp', \tag{2.52}$$

$$F_0(p) = e^{-\delta V/U_{th}}F_+(p_+(p)) + F(p). \tag{2.53}$$

The approximate value θ_Q^M is often referred to as the Marshak approximation. The more precise approximate value θ_Q^{GK} will be referred to as the Golse–Klar approximation. In the case of a relaxation time operator ((2.22) with (2.23)), ℓ_i is given by (2.46). For the same reason as for the albedo approximation, the leading order contribution to θ_Q is ϑ_1. This is why the numerical simulations (and particularly the current–voltage characteristic) show no difference between the Marshak and the Golse–Klar approximations (see below, Fig. 2).

3. DISCRETIZATION OF THE PROBLEM AND NUMERICAL RESULTS

We now solve the Schrödinger equation (2.2) on the bounded interval $[x_1, x_2]$ with boundary conditions (2.7) (for $p > 0$) and (2.8) (for $p < 0$). Here we treat the case $p > 0$ (the case $p < 0$ can be solved in the same way). First we remark that this system is equivalent to

$$\frac{d}{dx}\left(\frac{1}{m}y'(x)\right) = -\frac{2}{\hbar^2}(E_1 + e(V(x)-V_1))y(x), \tag{3.1}$$

$$y(x_2) = 1, \quad y'(x_2) = \frac{i}{\hbar}p_+(p). \tag{3.2}$$

ψ is related to y by $\psi = \gamma y$, where $\gamma = 2ip(\hbar y'(x_1) + ipy(x_1))^{-1}$.

We discretize problem (3.1), (3.2) by introducing a regular mesh of step $\xi_i = i\Delta x$ and setting $y_i \approx y(\xi_i)$. We obtain the discrete problem

$$\frac{1}{\Delta x}\left(\frac{1}{m_{i+\frac12}}y'_{i+\frac12} - \frac{1}{m_{i-\frac12}}y'_{i-\frac12}\right) = -\frac{2}{\hbar^2}(E + e(V_i - V_1))y_i, \tag{3.3}$$

with $y'_{i+\frac12} = (y_{i+1}-y_i)/\Delta x$ and $\xi_{i+\frac12} = \xi_i + \Delta x/2$, $m_{i+\frac12} \approx m(\xi_{i+\frac12})$. The matching conditions for ψ across a heterojunction interface (where m is discontinuous) are

$$\psi^- = \psi^+, \quad \frac{1}{m^-}\left(\frac{d\psi}{dx}\right)^- = \frac{1}{m^+}\left(\frac{d\psi}{dx}\right)^+,$$

where ψ^-, ψ^+, $(d\psi/dx)^-$, and $(d\psi/dx)^+$ denote the values of the wave-function and its derivatives on the left- and right-hand sides of the heterojunction, respectively. We deduce

that the equation

$$\frac{1}{\Delta x^2}\left(\frac{1}{m_{i+\frac{1}{2}}}y_{i+1}-\left(\frac{1}{m_{i+\frac{1}{2}}}+\frac{1}{m_{i-\frac{1}{2}}}\right)y_i+\frac{1}{m_{i-\frac{1}{2}}}y_{i-1}\right)=f(\xi_i,y_i), \tag{3.4}$$

with

$$f(x,y(x))=-\frac{2}{\hbar^2}(E_1+e(V(x)-V_1))y(x)$$

must be solved.

We use Stoermer's method [36], which consists in writing

$$\Delta_i=(y_{i+1}-y_i)/\Delta x,\quad i=0,\dots,N-1,$$
$$\Delta_N=y'(x_2)-\frac{m}{2}\Delta x f(x_2,y(x_2)).$$

We note that, in view of (3.2), Δ_N is a known quantity. Then, we have the iterations

$$\Delta_i=\frac{m_{i-\frac{1}{2}}}{m_{i+\frac{1}{2}}}\Delta_{i+1}-m_{i-\frac{1}{2}}\Delta x f_{i-1},$$
$$y_i=y_{i+1}-\Delta_i\Delta x,$$
$$y_0'=y'(x_1)=\Delta_1-m\frac{\Delta x}{2}f_0,$$

which allow us to compute Δ_i and y_i recursively. We also need the expression of $m(x)^{-1}$ $(\partial\psi/\partial x)$ in order to compute the quantum current from (2.12). We use the equation

$$\left(\frac{1}{m}y'\right)_i=\frac{1}{2}\left(\frac{1}{m_{i+\frac{1}{2}}}\Delta_{i+1}+\frac{1}{m_{i-\frac{1}{2}}}\Delta_i\right), \tag{3.5}$$

which, together with a standard quadrature formula, allows us to compute (2.12) numerically and to obtain an approximation of J_Q.

In order to solve the drift–diffusion equation, we choose the quasi-Fermi level formulation (V,φ), where φ is given by

$$n(x)=n(0)\exp\left(\frac{V-\varphi}{U_{th}}\right). \tag{3.6}$$

The continuity equation becomes

$$\frac{dJ}{dx}=0,\quad J=\frac{D}{U_{th}}\frac{d\varphi}{dx}n(x). \tag{3.7}$$

We obtain the boundary conditions for φ by imposing (2.17).

The drift–diffusion equations are solved by a classical finite volume approach, which for one-dimensional problems coincides with the famous box method (see, e.g., [41]). Using the Gummel approach [41], the Poisson equation is solved iteratively according to

$$-\frac{d}{dx}\left[\epsilon(x)\frac{d}{dx}V^{\ell+1}(x)\right]-q\frac{n^{\ell+1}}{U_{th}}(V^{\ell+1}-V^{\ell})=q(n_D(x)-n^{\ell+1}(x)), \tag{3.8}$$

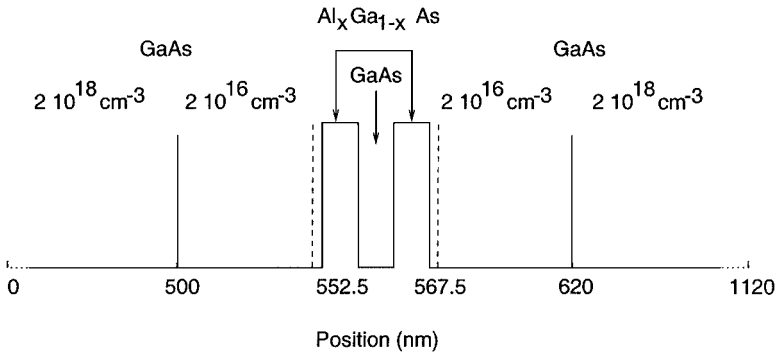

FIG. 1. The RTD geometry of [33].

where ℓ is the iteration index. The initial guess V^0 for the potential corresponding to the first bias is given by a linear function between 0 and L. We compute the solutions corresponding to a sequence of applied biases in increasing order. Once the solution for a given bias is computed, it is used as an initial guess in the iterations (3.8) for finding the next bias.

Gummel's method allows us to decouple the equations. Poisson's equation is solved first. Then, the obtained potential is substituted into the Schrödinger equation. From the reflection and transmission coefficients, the extrapolation constant θ_Q is computed. Then, the continuity equation (3.7) is resolved. The resulting density is then substituted back into Poisson's equation and the procedure is repeated until convergence is reached.

We shall consider two examples of resonant tunneling diode (RTD) structures dealt with in the literature. The first one has been treated by Mounaix *et al.* in [33]. The second one can be found in a paper by Kluksdahl *et al.* in [27]. The RTD geometry of Mounaix *et al.* [33] is depicted in Fig. 1. It is composed of a 5-nm undoped GaAs quantum well sandwiched between two 5-nm undoped $Al_{0.3}Ga_{0.7}As$ tunnel barriers. The double-barrier heterostructure is placed between two undoped thin cladding layers 2.5 nm in width and two 50-nm GaAs spacer layers with doping densities of $2\,10^{22}$ m^{-3}. Each GaAs contact layer is 500 nm wide, leading to a total device length of $L = 1120$ nm.

The physical quantities are chosen as follows. The double barrier height H is of 0.23 eV. The electron effective masses (relative to the vacuum electron mass) are given in Table I (where the indices 1 and 2 respectively refer to GaAs and $Al_{0.3}Ga_{0.7}As$ layers). The relative permittivity ϵ is constant througout the structure and is also given in Table I.

At room temperature $T = 300$ K, the mean collision time τ, the diffusitivity D, and the mean free path $\lambda = \tau v_{th}$ (with v_{th} given by (2.24)) are given in Table II below.

The mesh size is $\Delta x = 0.1$ nm in the quantum zone and $\Delta x = 0.5$ nm in the classical zone. We compute the scattering states of the Schrödinger equation for momenta p corresponding to energies up to $15\, k_B T$. They serve in the computation of the density $n(x)$ in the quantum zone Q and of the extrapolation constant θ_Q.

TABLE I
Masses and Permittivity

m_1	m_2	ϵ
0.067	0.092	12.4

TABLE II
Mean Collision Time τ, Diffusitivity D, and Mean Free Path λ

τ [s]	D [s^{-1} cm^2]	λ [nm]
$3.24\,10^{-13}$	$2.2\,10^{2}$	84.3

In Fig. 2 are displayed the RTD current–voltage characteristics obtained by means of the three approximate formulas for θ_Q: the albedo approximation (2.45), the Marshak approximation (2.47), and the Golse–Klar approximation (2.48). In this case, the classical–quantum interfaces are placed exactely at the $N^+ - N$ and $N - N^+$ junctions (500 and 620 nm). We observe that the Marshak and Golse–Klar approximations provide almost the same values of θ_Q. On the other hand, the albedo approximation leads to significantly different results. Since the Marshak and Golse–Klar formulae are the first iterations of a (formally) convergent sequence of approximations, that they give the fact similar results seems to be a good indication of their validity. Therefore, in the remainder of this section, we use the Marshak approximation. We refer to this case as the basic test case.

A comparison with [33] shows that our results differ in several respects. First, in [33], two current peaks are found in the current–voltage characteristic: a broad, flat one around 0.26 V and a narrow, sharp one around 0.32 V. We find only one peak around 0.25 V. Second, our values of the current are a factor of 2 below those of [33]. This last difference can easily be explained by the fact that our model is highly collisional (at least in the classical region) while that in [33] is collisionless. However, there are other major differences between our models, which can explain the different shapes of the current–voltage characteristics. In [33], the authors compute the potential and the wave-function in a decoupled way: the potential is first obtained via a Thomas–Fermi approximation of the density. Then, the

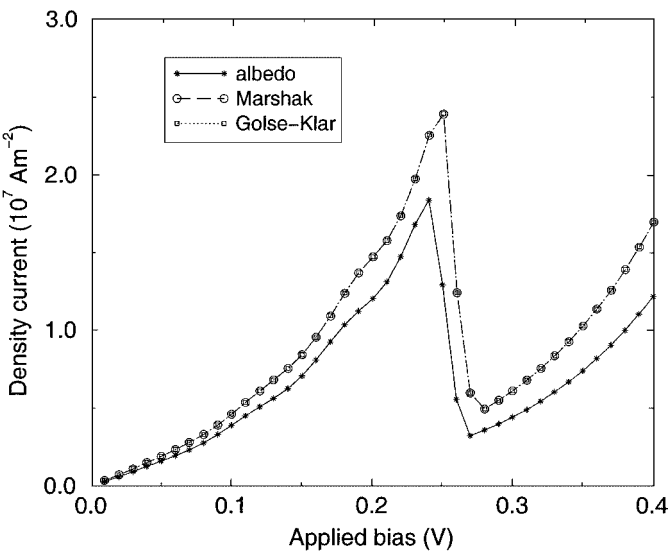

FIG. 2. Current–voltage characteristics obtained through the three approximations of the extrapolation length θ_Q.

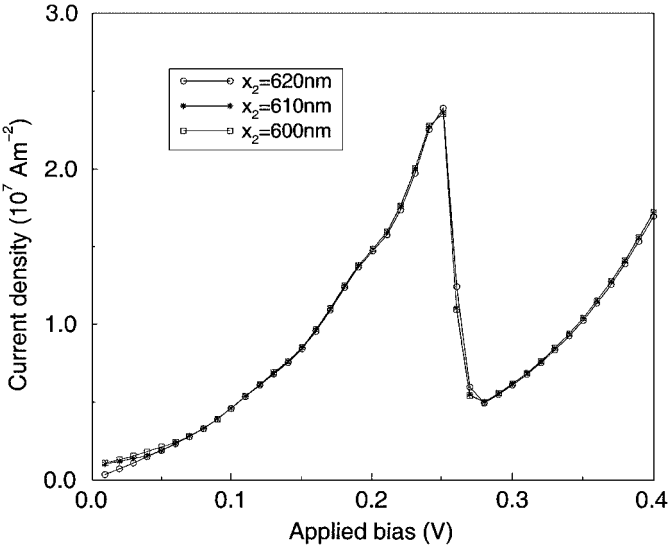

FIG. 3. Current–voltage characteristics when the x_2 interface is moved towards the left (from the basic case $x_2 = 620$ nm).

wave-functions, transmission coefficients, and eventually current are calculated by solving the Schrödinger equation in this given potential. There is no retroaction of the quantum calculation onto the potential shape. Our model instead is fully self-consistent. This may explain the observed differences between the numerical results.

Now, we investigate the influence of the position of classical–quantum interfaces x_1 and x_2 (cf. Figs. 3 to 6). These figures show that the results are quite insensitive to the position of the right interface x_2, but that the choice of the left interface x_1 is crucial. In particular, this

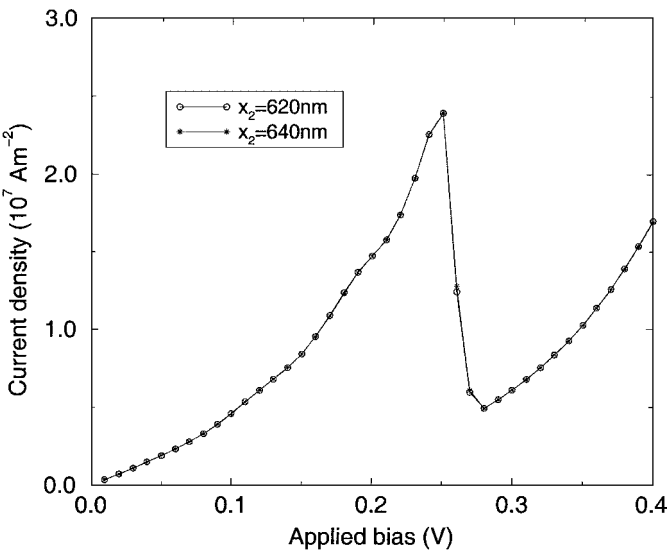

FIG. 4. Current–voltage characteristics when the x_2 interface is moved towards the right (from the basic case $x_2 = 620$ nm).

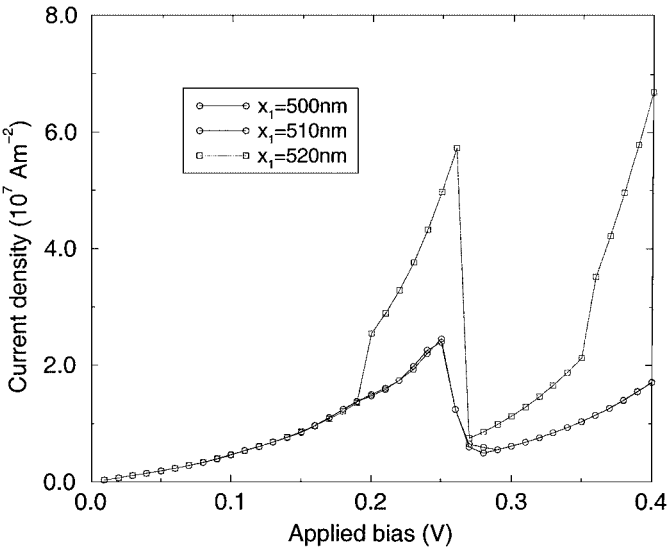

FIG. 5. Current–voltage characteristics when the x_1 interface is moved to the right (from the basic case $x_1 = 500$ nm).

interface cannot be chosen too close to the double barrier, otherwise the quantum resonances of the potential in the quantum region are not properly taken into acount. On the other hand, when the left interface is moved towards the source region, the results are not affected. The insensitivity of the results to the position of the right interface is easily explained by the fact that resonant particles are highly energetic in the drain region and therefore are equally well described by a classical or a quantum model. This is also seen on the formulae for the extrapolation constant, to which the major contributions are due to the right-going waves' transmission coefficients.

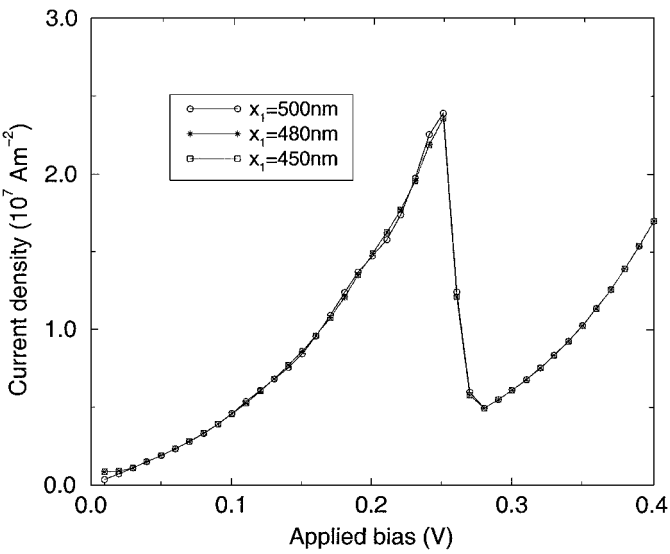

FIG. 6. Current–voltage characteristics when the x_1 interface is moved to the left (from the basic case $x_1 = 500$ nm).

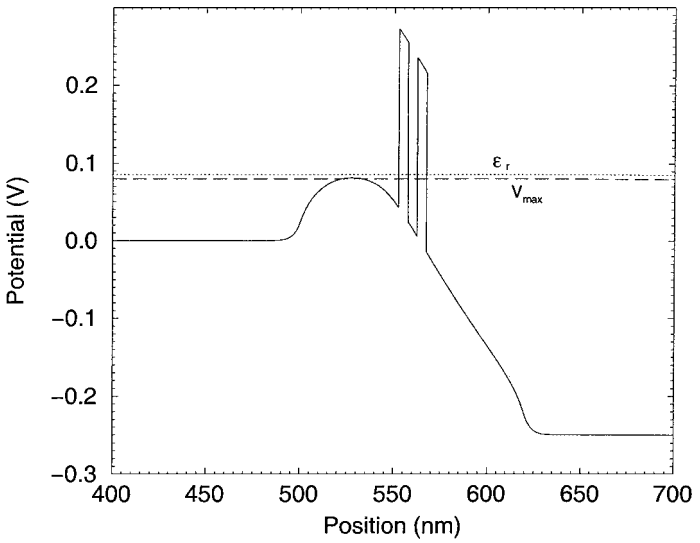

FIG. 7. Potential profile at the current peak bias (0.25 V).

Figure 7 displays the potential profile and Fig. 8 the carrier density profile for the voltage bias $V = 0.25$ V, corresponding to the current peak. The energy of the first resonance is indicated by the dotted line. The transmission coefficient as a function of the energy is shown in Fig. 9. In Fig. 9, the first transmission resonance appears with an energy $\varepsilon_r = V(x_1) + 0.064$ eV, and from Fig. 7, we have $V(x_1) = 0.023$ eV, which provides the resonant energy $\varepsilon_r = 0.087$ eV. It clearly appears that the resonant energy almost coincides with the maximum V_{max} of the potential in the region upstream from the double barrier (approximately located at $x = 530$ nm). For voltage biases $V = 0.15$ V or $V = 0.28$ V, which are respectively lower and higher than the peak bias, the resonance energy is respectively higher and lower than V_{max} (see Figs. 11 and 12).

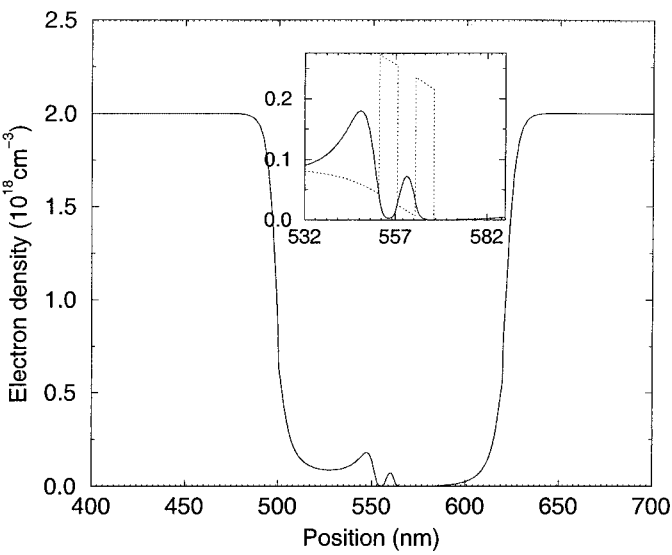

FIG. 8. Carrier density profile at the current peak bias (0.25 V).

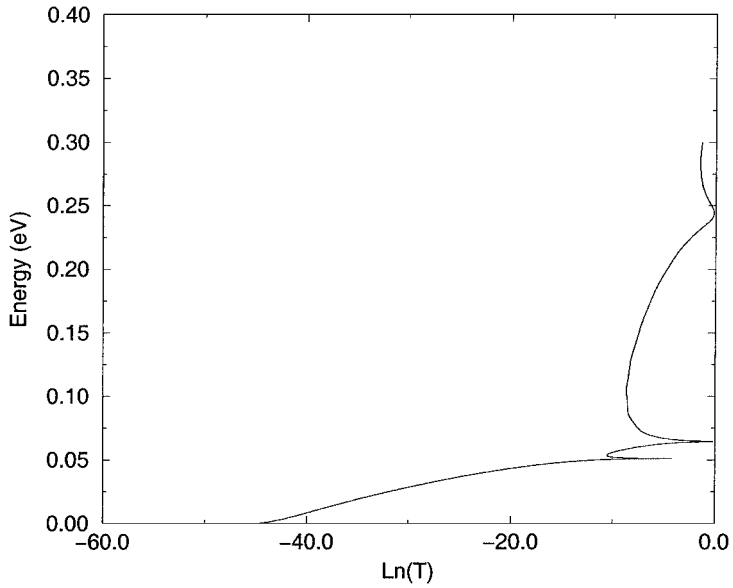

FIG. 9. Transmission probabilities for bias $V = 0.25$ V.

This observation is classical and can easily be interpreted as follows. The potential maximum V_{max} acts as a first filter on the transmitted particles: only those particles with energy ε lower than V_{max} can be transmitted. The distribution function of these particles is almost Maxwellian and therefore decreases exponentially as $\varepsilon - V_{max}$ increases. Then, the double barrier is a second filter, which only allows particles whose energy ε is equal to the transmission resonance energy ε_r to go through. The number of such particles is proportional to $\exp(-\frac{\varepsilon_r - V_{max}}{kT})$ for $\varepsilon_r > V_{max}$, and therefore, is maximal when

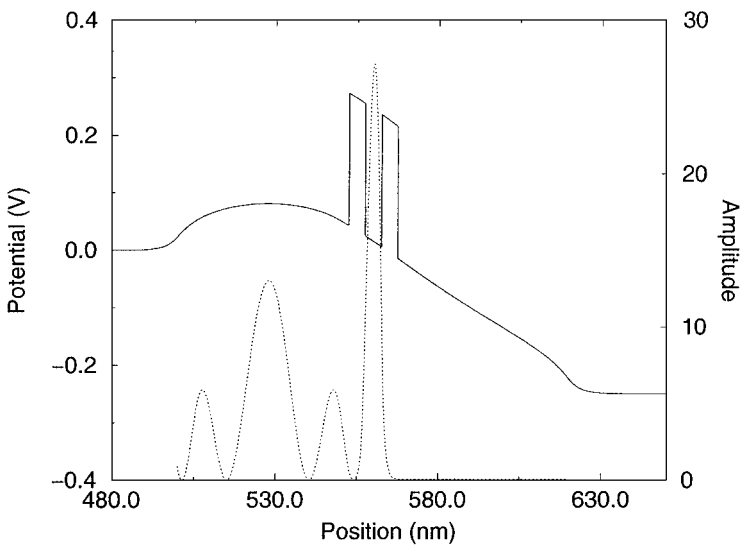

FIG. 10. Amplitude of the wave-function corresponding to the resonant energy $\varepsilon_r = 0.087$ eV (dotted curve) and potential profile (solid curve).

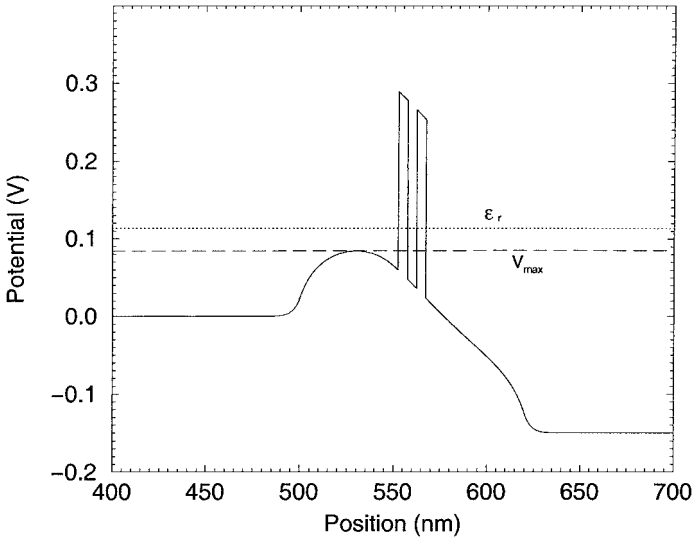

FIG. 11. Potential profile for bias $V = 0.15$ V.

$\varepsilon_r = V_{max}$. When $\varepsilon_r < V_{max}$, particles with a resonant energy ε_r first need to tunnel through the potential barrier V_{max}. Their number gets very small as soon as ε_r passes below V_{max}. This explains why the peak is observed when the transmission resonance energy coincides with V_{max}.

The density profile (Fig. 8) confirms that resonant particles actually tunnel through the first barrier and occupy the potential well between the two barriers (cf. inset). This phenomenon is also apparent on Fig. 10, which displays the wave-function corresponding to the resonant energy. There is a large occupation probability in the well, illustrated by a sharp peak of the wave-function. The other peaks from right to left are due to the broad potential well

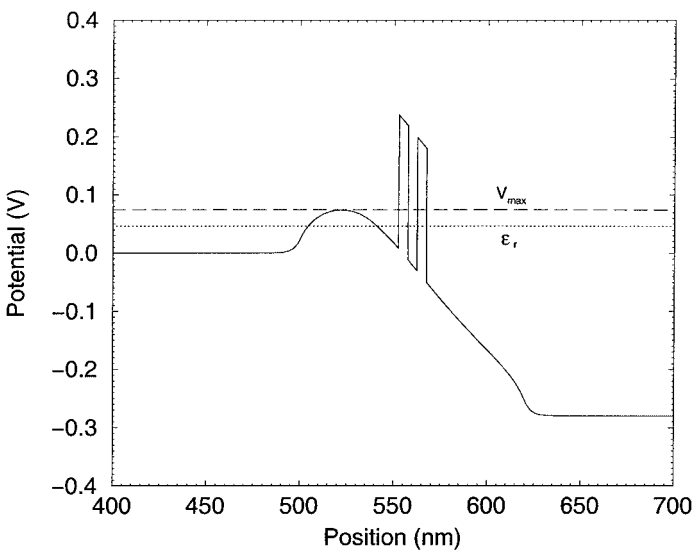

FIG. 12. Potential profile for bias $V = 0.28$ V.

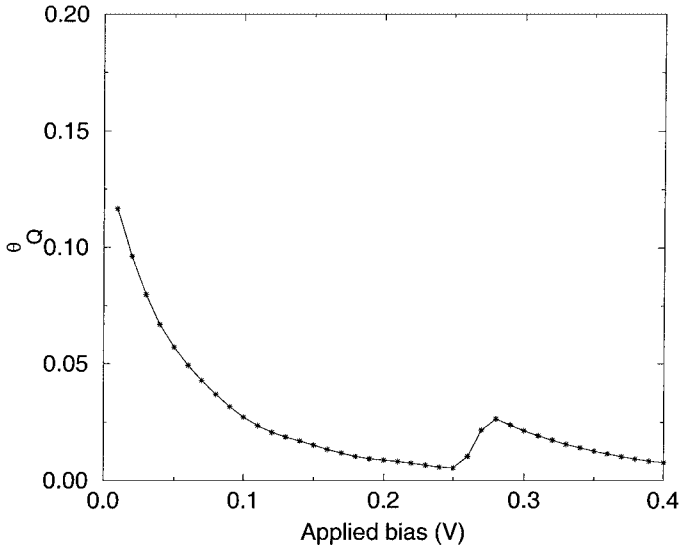

FIG. 13. Extrapolation constant as a function of the applied bias.

upstream of the double barrier (also seen in [33]) and to the cladding layers (which result in a discontinuity of the doping profile).

On Fig. 13, the curve representing the extrapolation constant as a function of the applied bias is shown. A sharp variation of the extrapolation constant around the current peak bias can be observed. It is a signature of the sharp variations of the transmission and reflection probabilities at resonance.

We have reduced the width of the potential barriers and well up to 1 nm, while simultaneously increasing the height of the barriers up to 1 eV, without observing any convergence problems or any kind of ill-behavior of the model. The results will be reported in future work [18]. In our opinion, this is an indication of the robustness of the method, which proves to be well suited to a wide variety of RTD designs.

Now, we would like to point out a limitation of the present model. Relaxation mechanisms occurring in the quantum region, such as phonon collisions, are not taken into account. However, they may contribute significantly to the physical process. Indeed, in the present

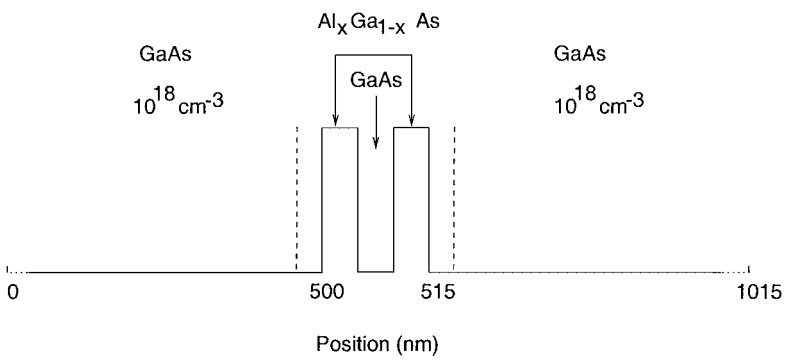

FIG. 14. The RTD geometry of [27].

TABLE III
Physical Parameters for the Test Case of [27]

m	ε_1	ε_2	H [eV]	τ (s)	T (K)
0.069	13.1	12.3	0.3	$1.177\,10^{-13}$	300

model, energy levels corresponding to the triangular potential well lying in front of the first barrier can only be fed by tunneling, whereas in an actual device, collision mechanisms may transfer a significant number of particles from higher energy states to these levels. At certain values of the applied bias, the tunneling current associated with these states could be larger than what the present model predicts. Therefore, a more accurate physical treatment of the problem would have to account for relaxation mechanisms and would most likely produce slightly different predictions for the transmission resonance and the peak bias. This point will be investigated in future work [18].

Next, we investigate the RTD geometry of [27] (see Fig. 14). It is composed of a 5-nm GaAs quantum well sandwiched between two 5-nm AlGaAs tunnel barriers. The double-barrier heterostructure (DBH) is sandwiched between two thin cladding layers 5 nm wide and two 495-nm-wide GaAs spacer layers. The DBH and the cladding layers are doped at 10^{21} m^{-3} while the spacer layer is doped at 10^{24} m^{-3}. The total length of the device is $L = 1015$ nm. We note that the total length simulated in [27] was shorter (65 nm), but this was probably due to numerical constraints.

The choice of physical constants is summarized in Table III (where H is the double-barrier height).

Figure 15 shows the current–voltage characteristics obtained with a fixed position of the second interface ($x_2 = 530$ nm) and various choices for the first interface ($x_1 = 490$ nm, $x_1 = 480$ nm, and $x_1 = 470$ nm). Paradoxically, when the x_1 interface is moved to the left

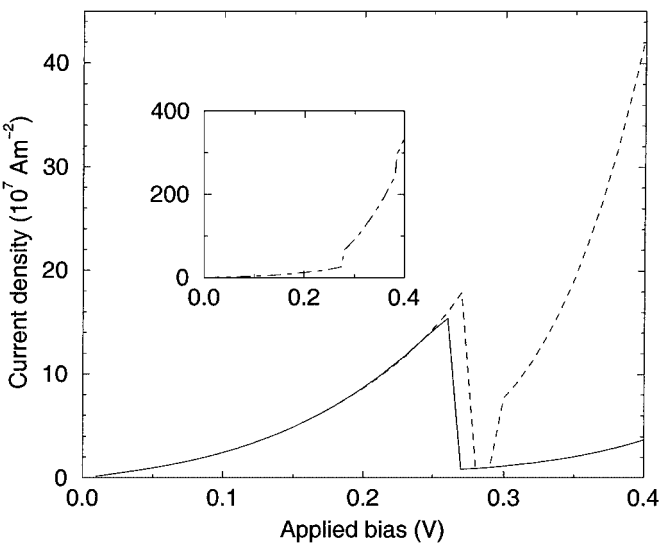

FIG. 15. Comparison of the current–voltage characteristics for the case of [27] with $x_1 = 490$ nm (solid line), $x_1 = 480$ nm (dashed line), and $x_1 = 470$ nm (dotted-dashed line in the inset). In these simulations, $x_2 = 530$ nm.

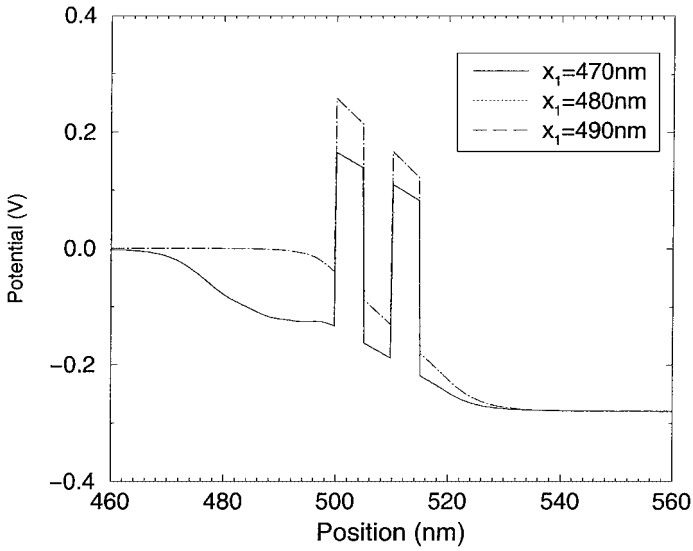

FIG. 16. Potential profiles for a voltage bias $V = 0.28$ V with the three choices of x_1.

(and therefore, when the size of the quantum region is increased), the results deteriorate dramatically. The results with $x_1 = 490$ nm compare well with those of [27] which are obtained via a numerical resolution of the relaxation-time Wigner equation. When $x_1 = 480$ nm and when $x_1 = 470$ nm, the peak-current reaches nonphysical values. This is easily explained by looking at the potential curves (Fig. 16), which exhibit a nonphysical deepening in the region upstream of the double barrier.

An interpretation of this behavior is found by considering the influence of collisions. Indeed, our treatment of the quantum region is collisionless. Therefore, as the quantum zone broadens, the treatment of collisions deteriorates. The nonphysical behavior of the current–voltage characteristic can be linked to the fact that collisions are neglected in too large a region of the device close to the double barrier. This interpretation is supported by the observation made in [27] that, when the relaxation-time Wigner equation is replaced by a conventional Schrödinger–Poisson solver (without any account of collisions), the potential curves display a nonphysical deepening in the whole device region. The collisions are essential to maintain the device close to a thermodynamical equilibruim. Neglecting them in too large a region results in nonphysical behavior.

4. CONCLUSION

In this paper, we have investigated a methodology to couple drift–diffusion and quantum models of electron transport in semiconductors in a one-dimensional stationary framework. The coupling methodology follows from the theory of boundary layers. The model has been numerically implemented and validated against two test cases in the literature. An adequate choice of the positions of the interfaces between the classical and quantum regions leads to good numerical results. The phenomena that affect the numerical results when the interfaces are moved have been analyzed.

Extension of the present work to multidimensional situations and to time-dependent problems is in progress [6].

5. APPENDIX A

From Kinetic to Drift–Diffusion Models by the Diffusion Approximation

In this appendix, for the reader's convenience, we provide the details that were omitted in Section 2.3.1. The rigorous derivation of the drift–diffusion model from the Boltzmann equation can be found in [25, 35] and other works. Formal derivations can be found in earlier works (see, e.g., [14, 39]). Here, we stay at the level of the formal derivation. However, we show that, formally, the drift–diffusion model is a second-order approximation of the Boltzmann equation in terms of the scaled mean free path. This will turn to be important in the next section for the obtention of the transmission conditions through the quantum zone.

We start with the properties of the collision operator Q (2.22). We note

$$\sigma(x, p) = \int_{\mathbb{R}} S(x, p, p') M(p')\, dp',$$

and we assume that there exist two positive constants σ_1 and σ_2 such that

$$0 < \sigma_1 < \sigma(x, p) \le \sigma_2, \quad \forall (x, p) \in C \times \mathbb{R}.$$

We also assume that $S(x, p, p') > 0$ for all (x, p, p'). Finally, we suppose that

$$Q(f)(-p) = Q(\check{f})(p), \tag{5.1}$$

where $\check{f}(p) = f(-p)$. It is easy to show that (5.1) is equivalent to $S(x, p, p') = S(x, -p, -p')$. The collision operator Q operates on the p variable only. Therefore, we introduce the space of square integrable functions of p for the measure $M^{-1}(p)\, dp$,

$$X = \left\{ f : \int_{\mathbb{R}} |f|^2 M^{-1}\, dp < \infty \right\},$$

which is a Hilbert space when equipped with the inner product

$$\langle f, g \rangle_X = \int_{\mathbb{R}} f g M^{-1}\, dp.$$

We also introduce the projection operator Π onto the Maxwellians:

$$(\Pi f)(p) = \langle f, M \rangle_X M(p) = \left(\int_{\mathbb{R}} f(p)\, dp \right) M(p).$$

The following lemma [35] summarizes the properties of Q as an operator on X.

LEMMA 5.1.

(i) $-Q$ *is a bounded, self-adjoint, nonnegative operator on* X.

(ii) *Its null space* $N(Q) = \{f \in X,\ Q(f) = 0\}$ *is a one-dimensional vector space, spanned by the Maxwellians*:

$$N(Q) = \{C M(p),\ C \in \mathbb{R}\}. \tag{5.2}$$

(iii) *Its range* $R(Q) = \{g \in X,\ \exists f \in X \text{ such that } Q(f) = g\}$ *is characterized by*

$$R(Q) = (N(Q))^{\perp}, \tag{5.3}$$

or

$$g \in R(Q) \Leftrightarrow \Pi g = 0 \Leftrightarrow \int_{\mathbb{R}} g(p)\,dp = 0. \tag{5.4}$$

(iv) *Let* $g \in R(Q)$. *Then, the function* $f \in X$ *such that* $Q(f) = g$ *is unique if* f *is constrained to satisfy* $\Pi f = 0$. *We denote it* $f = Q^{-1}(g)$. *The space of solutions is* $f + N(Q)$.

(v) $Q^{-1}(g)$ *has the same parity as* g (*i.e.*, *is even* (*respectively odd*) *when* g *is even* (*respectively odd*)).

We now consider the Boltzmann equation (2.21). Diffusion limits for stationary problems exhibit some pathologies. It is therefore easier to investigate a time-dependent problem or to substitute the time derivative with a damping term λf (with a constant damping coefficient $\lambda > 0$), which can be viewed as the Laplace transform of it. Moreover, we are ultimately interested in deriving the transmission conditions (2.15), (2.16) for which the presence of this additional term is indifferent. Therefore, we consider a damped equation of the form

$$\lambda f + \frac{p}{m}\frac{\partial f}{\partial x} + e\frac{dV}{dx}\frac{\partial f}{\partial p} = Q(f), \quad x \in \mathbb{R}, \quad p \in \mathbb{R}. \tag{5.5}$$

We disregard the boundary conditions for the time being and consider the problem for $x \in \mathbb{R}$.

The diffusion approximation for evolution problems consists in looking at space scales of order α^{-1} times the collision mean free path and at time scales of order α^{-2} times the mean collision time. In the present stationary situation, it amounts to rescaling the problem by changing λ into $\alpha^2\lambda$ and x into x/α. Therefore, (5.5) becomes

$$\lambda f^{\alpha} + \alpha^{-1}\left(\frac{p}{m}\frac{\partial f^{\alpha}}{\partial x} + e\frac{dV}{dx}\frac{\partial f^{\alpha}}{\partial p}\right) = \alpha^{-2}Q(f^{\alpha}), \quad x \in \mathbb{R}, \quad p \in \mathbb{R}. \tag{5.6}$$

In the following theorem, it is shown that in the limit $\alpha \to 0$, the solution of (5.6) converges to that of the (damped) drift–diffusion model.

THEOREM 5.2 (*formal*).

(i) f^{α} *tends to* $n(x,t)M$ *when* $\alpha \to 0$ *where* n *satisfies the* (*damped*) *stationary drift–diffusion model*,

$$\lambda n + \frac{dj}{dx} = 0, \tag{5.7}$$

$$j = -D(x)\left(\frac{dn}{dx} - n\frac{d}{dx}\left(\frac{V}{U_{th}}\right)\right), \tag{5.8}$$

with $D(x) > 0$ *given by* (2.27).

(ii) *n is formally a second-order approximation of n^α, i.e.,*

$$n^\alpha - n = O(\alpha^2), \quad n^\alpha(x,t) = \int_{\mathbb{R}} f^\alpha(x,v)\,dv, \tag{5.9}$$

(iii) *We have the expansion*

$$f^\alpha = f^0 + \alpha f^1 + O(\alpha^2), \quad f^0 = n(x,t)M(p), \quad f^1 = \ell(p)j,$$

where ℓ is given by (2.29).

Proof (*formal*). We only give the main steps of this proof, which is classical. We borrow this presentation from [15]. We introduce the Chapman–Enskog expansion

$$f^\alpha = f^0 + \alpha f^1 + \alpha^2 f^2 + \alpha^3 f^3 + O(\alpha^4) =: \tilde{f}^\alpha + O(\alpha^4), \tag{5.10}$$

where the f^i's are $O(1)$ but may depend on α. This allows us to choose $f^0 \in N(Q)$ and $f^i \in N(Q)^\perp$ for $i \geq 1$, or equivalently,

$$f^0(x,p,t) = n(x,t)M(p), \tag{5.11}$$

where n may also depend on α and

$$\Pi f^i = 0, \quad i = 1,2. \tag{5.12}$$

We calculate f^i, $i = 0, 3$ in such a way that $\tilde{f}^\alpha$ satisfies (5.6) up to $O(\alpha^2)$ terms, namely,

$$\lambda f^\alpha + \alpha^{-1} T(f^\alpha) - \alpha^{-2} Q(f^\alpha) = O(\alpha^2), \quad T(f) = \frac{p}{m}\frac{\partial f}{\partial x} + e\frac{dV}{dx}\frac{\partial f}{\partial p}. \tag{5.13}$$

We insert (5.10) in (5.13). Using (5.11) and (5.2), we are led to

$$\begin{aligned}\alpha^0((T - \Pi T)f^0 - Qf^1) + \alpha^1(\lambda(\mathrm{Id} - \Pi)f^0 + (T - \Pi T)f^1 - Qf^2)\\ + \alpha^2(\lambda f^1 + Tf^2 + \alpha^{-1}(\lambda \Pi f^0 + \Pi T f^1) + \alpha^{-2}\Pi T f^0 - Qf^3) = O(\alpha^3),\end{aligned} \tag{5.14}$$

where Id stands for the identity operator. In (5.14), we have used the remark after Eq. (5.10) and, for each term of the expansion, have subtracted its projection Π and compensated it by adding all these projections to the last term. Then, we set to 0 the various powers of α in (5.14). We summarize the results.

The order α^0 terms in (5.14) lead to $(T - \Pi T)f^0 = Qf^1$, which must be viewed as an equation for f^1. By construction, the solvability condition (5.4) is satisfied. This equation is easily solved and we find that f^1 is unique (in view of the constraint (5.12)) and given by $f^1 = \ell j$ with ℓ given by (2.29) and j by (5.8). In passing, we check that $\Pi T f^0 = 0$ because, f^0 being even, Tf^0 is odd.

Since, by construction, $(\mathrm{Id} - \Pi)f^0 = 0$, the order α^1 term leads to $(T - \Pi T)f^1 = Qf^2$, which again, is a solvable equation for f^2. We easily find the unique solution (satisfying (5.12))

$$f^2 = k^1 \frac{\partial j}{\partial x} + k^2 j,$$

with

$$k^1 = Q^{-1}\left(\frac{p}{m}\ell - M\right), \quad k^2 = Q^{-1}\left(\frac{p}{m}\frac{\partial \ell}{\partial x} + e\frac{dV}{dx}\frac{\partial \ell}{\partial p}\right).$$

The order α^2 term yields an equation for f^3 for which we only check the solvability (to guarantee the existence of f^3). Because $\Pi f^1 = 0$ (by (5.12)) and $\Pi\, Tf^0 = 0$ (by a remark above), the solvability equation reduces to

$$\lambda \Pi f^0 + \Pi\, T f^1 + \alpha \Pi\, T f^2 = 0. \tag{5.15}$$

Using Lemma 5.1 (v), we easily see that k^i, $i = 1, 2$ are even. Therefore, Tf^2 is odd and $\Pi\, Tf^2 = 0$. Easy computations lead to $\Pi f^0 = nM$ and $\Pi T\, f^1 = (\partial j/\partial x)M$. Therefore, (5.15) reduces to (5.7).

Now, from (5.13), it is readily seen that $\tilde{f}^\alpha$ is formally an order α^2 approximation of f^α. (One should not be confused by the order $O(\alpha^4)$ remainder in (5.10).) In fact, this remainder can only be proved of order α^2 because of the α^{-2} term in the equation). Because $\Pi f^i = 0$ for $i \geq 1$, (5.9) follows. The fact that D is positive is easily deduced from the nonnegativity of $-Q$ (see [35]). ■

6. APPENDIX B

Derivation of the Transmission Conditions for the Drift–Diffusion Model

In the present appendix, we consider the Boltzmann model (5.6) posed in the domain $C = C_1 \cup C_2$, $C_1 = (-\infty, x_1]$, $C_2 = [x_2, +\infty)$, together with the transmission conditions (2.33), (2.34) connecting the values of f^α at x_1 and x_2. We assume that the reflection–transmission coefficients of the quantum zone are known. Our goal is to show that, in order to maintain second-order accuracy in the diffusion approximation, the drift–diffusion model must be supplemented with the transmission conditions (2.15), (2.16), which, after rescaling, are written

$$j(x_1) = j(x_2) := \bar{j}, \tag{6.1}$$

$$n(x_1)e^{-V(x_1)/U_{th}} - n(x_2)e^{-V(x_2)/U_{th}} = \alpha\theta_Q \bar{j}, \tag{6.2}$$

with θ_Q as in Section 2.3. Since in the damped model the current may depend on x, we introduce the notation $\bar{j}$ to denote the common value (6.1). In the present analysis, we disregard the treatment of the boundary conditions at $x = 0$ and $x = L$, which is classical [3], and consider an infinite domain. The following approach mainly relies on [17] for its theoretical background.

We insert the Chapman–Enskog expansion (5.10) in (2.33) and stop the expansion at $O(\alpha^2)$, since we are aiming at an approximation of this order. This means that we are looking for f^0 and f^1 such that

$$\mathcal{B}\big(f_1^0, f_2^0\big) + \alpha\mathcal{B}\big(f_1^1, f_2^1\big) = O(\alpha^2), \tag{6.3}$$

where f_i^0, f_i^1 denote the limit values of f^0 and f^1 when $C_i \ni x \to x_1$. Similarly, n_i, j_i, ℓ_i, ... will denote the limit values of n, j, ℓ, ...

First, using the current-preservation property (2.36), the evenness of f^0 and f^2, and the fact that $\int \ell p/m\, dp = 1$, we deduce from (6.3) that

$$j_2 - j_1 = \int_{\mathbb{R}} f_2^1 \frac{p}{m}\, dp - \int_{\mathbb{R}} f_1^1 \frac{p}{m}\, dp = O(\alpha^2).$$

Therefore, up to a term of order α^2, we can impose the continuity of the current (6.1). We now derive (6.2).

First, let us notice that, in view of the last remark in Section 2.3.2, $\mathcal{B}(f_1^0, f_2^0) = 0$ if and only if n_1 and n_2 are linked through (2.37). The drift–diffusion model with transmission conditions (6.1), (2.37) is well posed. So far, these conditions only lead to a first-order approximation of the transmission conditions (2.33), since $\mathcal{B}(\tilde{f}_1^\alpha, \tilde{f}_2^\alpha) = O(\alpha)$. Additionally, there is no influence of the quantum region on the classical region (apart from through Poisson's equation). This is why we are looking for an order α^2 approximation.

Let us make it clear why (2.37) is not an order α^2 approximation. By linearity, we have

$$\mathcal{B}\big(f_1^1, f_2^1\big) = \bar{j}\mathcal{B}(\ell_1, \ell_2). \tag{6.4}$$

In general, it is not true that $\mathcal{B}(\ell_1, \ell_2) = 0$ (even when $\ell_1 = \ell_2$, which is the case as soon as $S(x_1, p, p') = S(x_2, p, p')$). To overcome this problem, we must introduce an internal layer corrector, based on the solution of the Milne problem (2.38), (2.39). For such a problem, we can show a general statement:

THEOREM 6.1.

(i) *Problem* (2.38)–(2.39) *with* $\ell_i = 0$, $i = 1, 2$ *admits a one-dimensional space of solutions consisting of*

$$\theta_i = C_i M \text{ on } \Theta_i \times \mathbb{R}, \tag{6.5}$$

where the two constants C_i *are linked by* (2.37).

(ii) *When* $\ell_i \neq 0$, *problem* (2.38)–(2.39) *has a bounded solution iff* ℓ_1 *and* ℓ_2 *satisfy the following flux conservation relation*:

$$\int_{\mathbb{R}} \ell_1\, p\, dp = \int_{\mathbb{R}} \ell_2\, p\, dp. \tag{6.6}$$

In this case, the solution is unique up to the addition of a solution of the form (6.5) *of the homogeneous problem.*

(iii) θ_i *has vanishing flux*:

$$\int_{\mathbb{R}} \theta_i\, p\, dp = 0, \quad \forall x \in \Theta_i. \tag{6.7}$$

(iv) *We have*

$$\theta_i \to n_{\theta_i}^\infty M \quad \text{as } x \to (-1)^i \infty, \tag{6.8}$$

where $n_{\theta_i}^\infty$ *is a constant and the convergence is exponentially fast. The constant*

$$\theta = e^{-V_2/U_{th}} n_{\theta_2}^\infty - e^{-V_1/U_{th}} n_{\theta_1}^\infty \tag{6.9}$$

does not depend on the choice of the solution and is uniquely determined by the data. It is called the extrapolation constant.

The existence theory for half-space problems of kinetic theory can be found in [3]. The theory of double-sided Milne problems such as (2.38)–(2.39) can be found in [17]. The proof of Theorem 6.1 can easily be adapted from [17]. We summarize the most important points of it at the end of this section. It is easy to check that (6.6) is satisfied for ℓ_i given by (2.29) since $\int \ell_i(p)p\,dp/m = 1$ by construction. Therefore, the existence and uniqueness (up to the addition of a solution of the homogeneous problem) of the solution of the Milne problem is guaranteed.

We are now able to prove:

THEOREM 6.2. *Second-order transmission conditions for the drift–diffusion model* (5.7)–(5.8) *are given by* (6.1), (6.2).

Remark 6.1. A sufficient condition which guarantees that problem (5.7)–(5.8) with transmission conditions (6.1), (6.2) is well posed is $\theta_Q > 0$. Indeed, after some easy computations, one obtains formally that

$$\lambda\left(\int_{-\infty}^{x_1} + \int_{x_2}^{\infty}\right)\frac{1}{2}|n(x)|^2 e^{-V/U_{th}}\,dx + \alpha\theta_Q|\bar{j}|^2 + \left(\int_{-\infty}^{x_1} + \int_{x_2}^{\infty}\right)D\left|\left(\partial_x n - n\partial_x\left(\frac{V}{U_{th}}\right)\right)\right|^2 e^{-V/U_{th}}dx = 0.$$

If $\theta_Q > 0$, all terms of the sum are positive, which allows us to apply the Lax–Milgram theorem to find a solution. Details are left to the reader. The positivity of θ_Q can be proved by means of a Darrozès Guiraud inequality (see [17]).

Proof of Theorem 6.2. From θ_i, we build the following internal layer corrector:

$$\chi_i^\alpha = -\bar{j}\big(\theta_i^\alpha - n_{\theta_i}^\infty M\big). \tag{6.10}$$

Because of (2.38), (2.39), (6.8), χ_i^α satisfies the Boltzmann equation (5.6) up to terms of order $\exp -(C|x - x_i|/\alpha)$ which are negligible away from a very tiny region about x_1 or x_2. Furthermore, it satisfies the transmission condition, thanks to (6.4) and (2.39):

$$\mathcal{B}\big(f_1^1 + \chi_1^\alpha, f_2^1 + \chi_2^\alpha\big) = \bar{j}\mathcal{B}\big(n_{\theta_1}^\infty M, n_{\theta_2}^\infty M\big). \tag{6.11}$$

Then, we modify the Chapman–Enskog expansion (5.10) slightly and write

$$f^\alpha = f^0 + \alpha(f^1 + \chi^\alpha) + \alpha^2 f^2 + \alpha^3 f^3 + O(\alpha^4) =: \bar{f}^\alpha + O(\alpha^4). \tag{6.12}$$

Inserting (6.12) in the Boltzmann equation (5.6) shows that f^α is formally an approximate solution of order $O(\alpha^2 + \alpha\exp -(C(|x - x_1| + |x - x_2|)/\alpha))$ and stays $O(\alpha^2)$ away from a tiny region about $[x_1, x_2]$.

Now, because of (6.11), $\bar{f}^\alpha$ satisfies the following transmission conditions:

$$\begin{aligned}\mathcal{B}\big(\bar{f}_1^\alpha, \bar{f}_2^\alpha\big) &= \mathcal{B}\big(f_1^0, f_2^0\big) + \alpha\mathcal{B}\big(\big(f_1^1 + \chi_1^\alpha\big), \big(f_2^1 + \chi_2^\alpha\big)\big) + O(\alpha^2)\\ &= \mathcal{B}\big(\big(n_1 + \alpha\big(\bar{j}n_{\theta_1}^\infty\big)\big)M, \big(n_2 + \alpha\big(\bar{j}n_{\theta_2}^\infty\big)\big)M\big) + O(\alpha^2).\end{aligned} \tag{6.13}$$

Therefore, in view of the last remark in Section 2.3.2, the second-order transmission condition is written

$$\left(n_1 + \alpha\left(\bar{j} n_{\theta_1}^{\infty}\right)\right) e^{-V_1/U_{th}} - \left(n_2 + \alpha\left(\bar{j} n_{\theta_2}^{\infty}\right)\right) e^{-V_2/U_{th}} = 0, \tag{6.14}$$

which can also be written according to (6.2), which concludes the proof. ∎

We now sketch some points of the proof of Theorem 6.1.

Proof of Theorem 6.1 (sketch). First, suppose that θ_i is a bounded solution of (2.38)–(2.39). Then, integrating (2.38) with respect to p leads to

$$\partial_x J_i(x) = 0, \quad J_i(x) = \int_{\mathbb{R}} \theta_i \frac{p}{m}\, dp. \tag{6.15}$$

Therefore, $J_i(x) = J_i$ is a constant.

Using Green's formula and the self-adjointness of Q, we observe that

$$\int_{\mathbb{R}} Q(f) h M^{-1}\, dp = \int_{\mathbb{R}} f\, Q(h) M^{-1}\, dp = -\int_{\mathbb{R}} f \frac{p}{m}\, dp.$$

Therefore, multiplying (2.38) by hM^{-1} and integrating with respect to p, we obtain

$$\partial_x k_i + J_i = 0, \quad k_i(x) = \int_{\mathbb{R}} \frac{p}{m} \theta_i\, h\, M^{-1}\, dp. \tag{6.16}$$

Since we look for a bounded θ_i as $x \to (-1)^i \infty$, k_i must also stay bounded (provided there is no integrability problem with respect to p), which implies

$$J_i(x) = 0, \quad k_i(x) = k_i = \text{ constant}, \quad \forall x \in \Theta_i, \tag{6.17}$$

and leads to point (iii). Given that the transmission condition (2.33) preserves the flux through the quantum zone (2.36), we deduce that, for a bounded solution to exist, relation (6.6) must hold. This explains the "only if" part of statement (ii).

Property (iv) is classical for Milne problems [3] and expresses the fact that away from the quantum region the solution converges to an equilibrium. Parts (i) and the "if" part of (ii) follow from the Fredholm techniques of [17]. Details are left to the reader. ∎

For future use, we note that taking the limit $x \to (-1)^i \infty$ and using (6.8), we have

$$k_i = n_{\theta_i}^{\infty} D_i, \tag{6.18}$$

where $D_i = D(x_i)$. The following expression of θ_Q follows:

$$\begin{aligned} \theta_Q &= e^{-V_2/U_{th}} \frac{k_2}{D_2} - e^{-V_1/U_{th}} \frac{k_1}{D_1} \\ &= e^{-V_2/U_{th}} \int_{\mathbb{R}} \theta_2\, \ell_2 \frac{p}{m} \frac{dp}{M} - e^{-V_1/U_{th}} \int_{\mathbb{R}} \theta_1\, \ell_1 \frac{p}{m} \frac{dp}{M}. \end{aligned} \tag{6.19}$$

7. APPENDIX C

Approximation of the Albedo Operator

Proof of formula (2.44). We first write the transmission condition (2.39) with the assumption (2.43) according to

$$\begin{aligned}
&\big(\theta_1(p) - n_{\theta_1}^- M(p)\big) - (\ell_1(p) - \ell_1(-p)) \\
&\quad = \big(n_{\theta_2}^- e^{-\delta V/U_{th}} - n_{\theta_1}^-\big) T(-p) M(p) + T(-p)\ell_1(-p) \\
&\qquad - T(-p_+(p))\ell_2(-p_+(p)), \quad p < 0, \qquad (7.1)\\
&\big(\theta_2(p) - n_{\theta_2}^- M(p)\big) - (\ell_2(p) - \ell_2(-p)) \\
&\quad = \big(n_{\theta_1}^- - n_{\theta_2}^- e^{-\delta V/U_{th}}\big) T(p_-(p)) M(p_-(p)) + T(-p)\ell_2(-p) \\
&\qquad - T(p_-(p))\ell_1(p_-(p)), \quad p > p_\delta, \qquad (7.2)\\
&\big(\theta_2(p) - n_{\theta_2}^- M(p)\big) - (\ell_2(p) - \ell_2(-p)) = 0, \quad 0 < p < p_\delta, \qquad (7.3)
\end{aligned}$$

where we have used the fact that $M(p_+(p)) = e^{-\delta V/U_{th}} M(p)$ and $M(p_-(p)) = e^{\delta V/U_{th}} M(p)$. We note the relations

$$\int_{-\infty}^{0} \big(\theta_1 - n_{\theta_1}^- M(p)\big) p\, dp = 0, \quad \int_{-\infty}^{0} (\ell_1(p) - \ell_1(-p)) p\, dp = \int_{\mathbb{R}} \ell_1(p) p\, dp = m, \qquad (7.4)$$

as well as the similar ones (with integration on $[0, \infty)$) for θ_2 and ℓ_2. Moreover, using the changes of variables $\bar{p} = -p_+(p)$ and $\bar{p} = p_-(p)$, we get the two relations

$$\int_{-\infty}^{0} \varphi(-p_+(p)) p\, dp = \int_{-\infty}^{-p_\delta} \varphi(p) p\, dp, \quad \int_{p_\delta}^{\infty} \varphi(p_-(p)) p\, dp = \int_{0}^{\infty} \varphi(p) p\, dp, \qquad (7.5)$$

for any function φ.

Now, multiplying (7.1) by p/m, integrating with respect to p over $(-\infty, 0]$, and using relations (7.4), (7.5), we obtain

$$n_{\theta_2}^- e^{-\delta V/U_{th}} - n_{\theta_1}^- = \left(\int_0^\infty T M \frac{p}{m}\, dp\right)^{-1} \left(1 - \int_0^\infty [\ell_1(p) + \ell_2(p_+(p))]\, T \frac{p}{m}\, dp\right). \qquad (7.6)$$

It is readily observed that using eqs. Eqs. (7.2) and (7.3) instead of (7.1) would lead to the same result. Therefore, the approximate solution as well as the exact one is defined uniquely up to the addition of Maxwellians $n_i M$, the densities n_i of which are related through (2.37).

Now, with (2.43), we note that

$$\frac{k_1}{D_1} = \int_{-\infty}^{0} \ell_1 \theta_1 \frac{p}{m} \frac{dp}{M} + \frac{n_{\theta_1}^-}{2},$$

and similarly for k_2/D_2 with the integral on $[0, \infty)$. We also note that the functions ℓ_i are odd while $\ell_1 M^{-1} p/m$ are even. Therefore, multiplying (7.1) by $\ell_1 M^{-1} p/m$ and integrating over $(-\infty, 0]$ yields

$$\frac{k_1}{D_1} - n_{\theta_1}^- = -2\int_0^\infty (\ell_1)^2 \frac{p}{m}\frac{dp}{M} + \left(n_{\theta_2}^- e^{-\delta V/U_{th}} - n_{\theta_1}^-\right)\int_0^\infty \ell_1 T \frac{p}{m} dp + \int_0^\infty (\ell_1)^2 T \frac{p}{m}\frac{dp}{M} + \int_0^\infty \ell_1(p)\,\ell_2(p_+(p))\,T\frac{p}{m}\frac{dp}{M}. \tag{7.7}$$

Similarly, using (2.9), the change of variable $\bar{p} = p_+(p)$, and the oddness of ℓ_2, we get

$$\frac{k_2}{D_2} - n_{\theta_2}^- = 2\int_0^\infty (\ell_2)^2 \frac{p}{m}\frac{dp}{M} + \left(n_{\theta_1}^- - n_{\theta_2}^- e^{-\delta V/U_{th}}\right)e^{\delta V/U_{th}}\int_0^\infty \ell_2(p_+(p))\,T\frac{p}{m}dp - e^{\delta V/U_{th}}\int_0^\infty (\ell_2(p_+(p)))^2\,T\frac{p}{m}\frac{dp}{M} - e^{\delta V/U_{th}}\int_0^\infty \ell_2(p_+(p))\,\ell_1(p)\,T\frac{p}{m}\frac{dp}{M}. \tag{7.8}$$

Then, multiplying (7.8) by $e^{-\delta V/U_{th}}$ and substracting (7.7), we obtain

$$e^{-\delta V/U_{th}}\frac{k_2}{D_2} - \frac{k_1}{D_1} = \left(n_{\theta_2}^- e^{-\delta V/U_{th}} - n_{\theta_1}^-\right)\left(1 - \int_0^\infty [\ell_1(p) + \ell_2(p_+(p))]\,T\frac{p}{m}dp\right) + 2\int_0^\infty \left((\ell_2)^2 e^{-\delta V/U_{th}} + (\ell_1)^2\right)\frac{p}{m}\frac{dp}{M} - \int_0^\infty [\ell_1(p) + \ell_2(p_+(p))]^2\,T\frac{p}{m}\frac{dp}{M}. \tag{7.9}$$

Then, inserting (7.6) into (7.9) and multiplying by $e^{-V_1/U_{th}}$ leads to (2.44), by virtue of (6.19). ■

Proof of the positivity of $\bar{\theta}_Q$ (2.45). We can write $\bar{\theta}_Q$ according to

$$\bar{\theta}_Q = e^{-V_1/U_{th}}\left(\int_0^\infty T M \frac{p}{m}dp\right)^{-1}\left(1 - \int_0^\infty [\ell_1(p) + \ell_2(p_+(p))]\,T\frac{p}{m}dp\right)^2 + 2\int_0^{p_\delta} (\ell_2)^2 e^{-V_2/U_{th}}\frac{p}{m}\frac{dp}{M} + e^{-V_1/U_{th}}\zeta,$$

with

$$\zeta = 2\int_0^\infty \left((\ell_2(p_+(p)))^2 + (\ell_1(p))^2\right)\frac{p}{m}\frac{dp}{M} - \int_0^\infty [\ell_1(p) + \ell_2(p_+(p))]^2\,T\frac{p}{m}\frac{dp}{M}.$$

To prove that $\bar{\theta}_Q > 0$, it is enough to show that the ζ is nonnegative. This follows easily from the facts that $[\ell_1(p) + \ell_2(p_+(p))]^2 \le 2[\ell_2(p_+(p))^2 + (\ell_1(p))^2]$ and $T \le 1$. ■

8. APPENDIX D

8.1. Golse–Klar Iterations

Principle of the Method

We recall that we are looking for the solution (θ_1, θ_2) of the Milne problem (2.38), (2.39). The solution such that $\theta_i M^{-1}$ is bounded is unique up to the addition of Maxwellians of constant densities in each Θ_i, related by (2.37). Furthermore, this solution has zero flux. In this section, we specialize to the case of a constant transition rate (2.23), so that (2.38) is written

$$\frac{p}{m}\frac{\partial \theta_i}{\partial x} + \tau_i^{-1}\big(\theta_i - n_{\theta_i} M\big) = 0, \quad p \in \mathbb{R}, \quad x \in \Theta_i, \tag{8.1}$$

where τ_i is the collision frequency in Θ_i and $n_\theta = \int \theta(p)\, dp$.

The first iteration consists in replacing problem (2.38), (2.39) by

$$\frac{p}{m}\frac{\partial \theta_i^1}{\partial x} + \tau_i^{-1}\big(\theta_i^1 - n_i^1 M\big) = 0 \tag{8.2}$$

$$\mathcal{B}\big(\theta_1^1(0, p) - \ell_1(p), \theta_2^1(0, p) - \ell_2(p)\big) = 0. \tag{8.3}$$

$$\theta_i^1 M^{-1} \text{ bounded on } \Theta_i, \tag{8.4}$$

$$n_i^1 \text{ constant on } \Theta_i \text{ and such that } \int_{\mathbb{R}} \theta_i^1(0, p)\, p\, dp = 0. \tag{8.5}$$

We note that if $(\theta_i^1, n_i^1)_{i=1,2}$ is a solution of (8.2), (8.5), then $(\theta_i^1 + C_i M, n_i^1 + C_i)$, where C_i are constants, is another solution if and only if the C_i are related by (2.37). It is easily shown that problem (8.2), (8.5) has a unique solution modulo this transformation (see below).

Suppose that a $(k-1)$-th order approximation has been constructed in the form of a series $\theta_i^1 + \theta_i^2 + \cdots + \theta_i^{k-1}$. Then, following Golse–Klar [24], we construct a k-th order solution by solving the problem

$$\frac{p}{m}\frac{\partial \theta_i^k}{\partial x} + \tau_i^{-1}\big(\theta_i^k - n_i^k(x) M\big) = -\tau_i^{-1}\big(n_i^{k-1}(x) - n_{\theta_i^{k-1}}(x)\big) M \tag{8.6}$$

$$\frac{\partial^2}{\partial x^2}(D_i n_i^k) - \tau_i^{-1}\big(n_i^{k-1}(x) - n_{\theta_i^{k-1}}(x)\big) = 0, \tag{8.7}$$

$$\mathcal{B}\big(\theta_1^k(0, p), \theta_2^k(0, p)\big) = 0. \tag{8.8}$$

$$\theta_i^k M^{-1} \text{ bounded on } \Theta_i, \tag{8.9}$$

$$n_i^k \text{ bounded on } \Theta_i \text{ and } \lim_{|x|\to\infty} n_i^k := n_i^{k\infty} \text{ such that } \int_{\mathbb{R}} \theta_i^k(0, p)\, p\, dp = 0\,. \tag{8.10}$$

Again, it is easily seen that problem (8.6), (8.10) has a unique solution, modulo the addition of a Maxwellian. The rationale for this method is that the density n_{th_i} in the collision operator is replaced by its approximation by the diffusion equation (8.7) (which has a constant solution at the first iteration). Then, a correction to this approximation is sought by solving the next order iteration. It is clear that, if these iterations converge, they do converge towards the solution of the Milne problem (2.38), (2.39). To our knowledge, the rigorous proof of the convergence of these iterations is still an open problem.

In this procedure, we are mostly interested in

$$\vartheta_k = \left(e^{-\delta V/U_{th}} n^{\infty}_{\theta_2^k} - n^{\infty}_{\theta_1^k}\right) \quad \text{with} \lim_{|x|\to\infty} \theta_i^k = n^{\infty}_{\theta_i^k} M,$$

because, to the k-th order, θ_Q is approximated by:

$$\theta_Q \approx \theta_Q^k = \sum_k \left(e^{-V_2/U_{th}} n^{\infty}_{\theta_2^k} - e^{-V_1/U_{th}} n^{\infty}_{\theta_1^k}\right) = e^{-V_1/U_{th}} \sum_k \vartheta_k.$$

Now, our aim is to explicitly compute the first and second iterates ϑ_1 and ϑ_2.

8.2. First Iteration

The explicit integration of (8.2) gives

$$\theta_1^1(x,p) = \begin{cases} \theta_1^{1+}(p) e^{-\frac{mx}{\tau_1 p}} + n_1^1 M\left(1 - e^{-\frac{mx}{\tau_1 p}}\right), & x \le 0, \quad p \le 0 \\ n_1^1 M, & x \le 0,\ p \ge 0, \end{cases} \tag{8.11}$$

where $\theta_1^{1\pm}(p) = \theta_1^1(0,p)$ for $\mp p \ge 0$. A similar formula is valid mutatis mutandis for θ_2^1 in terms of θ_2^{1+} with $\theta_2^{1\pm}(p) = \theta_2^1(0,p)$ for $\pm p \ge 0$.

The functions θ_i^{1+} are determined by means of the transmission condition (8.3), which in this case coincides with (7.1), (7.3) (changing $n_{\theta_i}^-$ into n_i^1). We know that the transmission condition (8.3) implies $\int \theta_i^1(0,p)\, pdp = \int \theta_2^1(0,p)\, pdp$. Therefore, to ensure (8.5), it is enough to ensure that only one of the fluxes is zero, for instance that of θ_1^1. Therefore, integrating (7.1) yields (7.6) (with, again, $n_{\theta_i}^-$ changed into n_i^1). Now, the asymptotic values of θ_i^1 as $|x| \to \infty$ are clearly given by n_i^1. Therefore, (7.6) gives rise to formula (2.49) for ϑ_1. Stopping the iterations at this point would lead to the so-called Marshak approximation, which is often considered too coarse.

8.3. Second Iteration

We now compute the second iterate (θ_i^2, n_i^2). We obtain

$$\theta_1^2(x,p) = \begin{cases} \theta_1^{2+}(p) e^{-\frac{mx}{\tau_1 p}} + \frac{m}{\tau_1 p} M \int_0^x e^{-\frac{m(x-y)}{\tau_1 p}} \left(n_1^2 - \left(n_1^1 - n_{\theta_1^1}\right)\right)(y)\, dy, & x \le 0,\ p \le 0 \\ \theta_1^{2-}(p) e^{-\frac{mx}{\tau_1 p}} + \frac{m}{\tau_1 p} M \int_0^x e^{-\frac{m(x-y)}{\tau_1 p}} \left(n_1^2 - \left(n_1^1 - n_{\theta_1^1}\right)\right)(y)\, dy, & x \le 0,\ p \ge 0, \end{cases} \tag{8.12}$$

where $\theta_1^{2-}(p)$ is determined in a such a way that $M^{-1}\theta_1^2$ is bounded on $(-\infty, 0]$. A similar formula is valid for θ_2^2 on $[0, \infty)$.

Now, we easily compute from (8.11),

$$\left(n_1^1 - n_{\theta_1^1}\right)(x) = -\int_{-\infty}^0 \left(\theta_1^{1+}(p) - n_1^1 M(p)\right) e^{-\frac{mx}{\tau_1 p}}\, dp, \tag{8.13}$$

and bounded solutions of (8.7) are readily found—

$$n_1^2 = n_1^{2\infty} - \int_{-\infty}^0 \left(\theta_1^{1+}(p) - n_1^1 M(p)\right) \frac{p^2}{p_{th}^2} e^{-\frac{mx}{\tau_1 p}}\, dp, \tag{8.14}$$

where the integration constant $n_1^{2\infty}$ will be determined later.

Inserting (8.13) and (8.14) into (8.12) leads to

$$\theta_1^2(x,p) = \begin{cases} \theta_1^{2+}(p)e^{-\frac{mx}{\tau_1 p}} + n_1^{2\infty}M\big(1-e^{-\frac{mx}{\tau_1 p}}\big) - M\int_{-\infty}^0 \big(\theta_1^{1+}(p') - n_1^1 M(p')\big) \\ \quad \times\big(\frac{p'^2}{p_{th}^2}-1\big)\big(e^{-\frac{mx}{\tau_1 p'}} - e^{-\frac{mx}{\tau_1 p}}\big)\frac{p'}{p'-p}\,dp', \quad x\le 0,\ p\le 0 \\ n_1^{2\infty}M - M\int_{-\infty}^0 \big(\theta_1^{1+}(p') - n_1^1 M(p')\big)\big(\frac{p'^2}{p_{th}^2}-1\big)e^{-\frac{mx}{\tau_1 p'}}\,\frac{p'}{p'-p}\,dp', \quad x\le 0,\ p\ge 0. \end{cases} \tag{8.15}$$

In (8.15), for $p \ge 0$, θ_1^{2-} has been eliminated by enforcing the boundedness constraint on θ_1^2. A similar expression can be obtained, mutatis mutandis, for θ_2^2. We note that θ_i^2 tends to $n_i^{2\infty}M$ as $|x|$ tends to ∞, so that ϑ_2 is given by

$$\vartheta_2 = e^{-\delta V/U_{th}} n_2^{2\infty} - n_1^{2\infty}. \tag{8.16}$$

We are now going to apply (8.8), (8.10) in order to find ϑ_2.

For that purpose, according to (8.15), we write

$$\theta_1^{2-}(p) = n_1^{2\infty}M - M\phi_1, \quad p>0; \quad \theta_2^{2-}(p) = n_2^{2\infty}M - M\phi_2, \quad p<0, \tag{8.17}$$

with

$$\phi_1(p) = \int_0^\infty \big(\theta_1^{1+}(-p') - n_1^1 M(p')\big)\left(\frac{p'^2}{p_{th}^2}-1\right)\frac{p'}{p'+p}\,dp', \quad p>0, \tag{8.18}$$

$$\phi_2(-p) = \int_0^\infty \big(\theta_2^{1+}(p') - n_2^1 M(p')\big)\left(\frac{p'^2}{p_{th}^2}-1\right)\frac{p'}{p'+p}\,dp', \quad p>0. \tag{8.19}$$

Because the transmission condition (8.8) is flux-preserving, in order to enforce condition (8.10) for both functions $\theta_i^2(0,p)$, it is enough to enforce it for only one of them, say $\theta_1^2(0,p)$. Then, integrating the first line of (2.34) with respect to $p\,dp$ and using (8.17) leads to

$$\vartheta_2 = \left(\int_0^\infty TM\frac{p}{m}\,dp\right)^{-1}\int_0^\infty TM\left[e^{-\delta V/U_{th}}\phi_2(-p_+(p)) - \phi_1(p)\right]\frac{p}{m}\,dp. \tag{8.20}$$

We now compute ϕ_i. We again use the fact that the functions θ_i^{1+} are determined by (7.1), (7.3) (changing $n_{\theta_i}^-$ into n_i^1). Writing (7.1) in terms of $-p'$ instead of p, multiplying by $(p'^2/p_{th}^2-1)\,p'/(p'+p)$ and integrating with respect to p' leads to

$$\phi_1(p) = \int_0^\infty \{-2\ell_1(p') + \vartheta_1 T(p')M(p') + T(p')[\ell_1(p') + \ell_2(p_+(p'))]\} \times\left(\frac{p'^2}{p_{th}^2}-1\right)\frac{p'}{p'+p}\,dp', \quad p>0. \tag{8.21}$$

Similarly for ϕ_2, using (7.2), (7.3) and the change of variables $p' = p_+(\bar{p}')$, we get

$$\phi_2(-p_+(p)) = \int_0^\infty \{2\ell_2(p_+(p')) - \vartheta_1 T(p')M(p') - T(p')[\ell_1(p') + \ell_2(p_+(p'))]\} \times \left(\frac{p_+(p')^2}{p_{th}^2} - 1\right) \frac{p'\,dp'}{p_+(p') + p_+(p)} + \int_0^{p_\delta} 2\ell_2(p') \left(\frac{p'^2}{p_{th}^2} - 1\right) \frac{p'\,dp'}{p' + p_+(p)}, \quad p > 0. \tag{8.22}$$

By inserting (8.21) and (8.22), we deduce 2.50, which concludes the proof. ■

ACKNOWLEDGMENTS

The authors thank Prof. N. Ben Abdallah for fruitful discussions and suggestions. This work has been supported by the TMR Network ERB FMBX CT97 0157 on "asymptotic methods in kinetic theory" of the European Community.

REFERENCES

1. P. N. Argyres, Quantum kinetic equations for electrons in high electric and phonon fields, *Phys. Lett. A* **171**, 373 (1992).
2. C. Bardos, F. Golse, and B. Perthame, The Rosseland approximation for the radiative transfer equations, *Commun. Pure Appl. Math.* **40**, 691 (1987) and **42**, 891 (1989).
3. C. Bardos, R. Santos, and R. Sentis, Diffusion approximation and computation of the critical size, *Trans. Am. Math. Soc.* **284**, 617 (1984).
4. N. Ben Abdallah, A hybrid kinetic-quantum model for stationary electron transport in a resonant tunneling diode, *J. Stat. Phys.* **90** (3–4), 627 (1998).
5. N. Ben Abdallah and P. Degond, On a hierarchy of macroscopic models for semiconductors, *J. Math. Phys.* **37**, 3306 (1996).
6. N. Ben Abdallah, P. Degond, and I. M. Gamba, Coupling one-dimensional time-dependent classical and quantum transport models, *J. Math. Phys.* **43**, 1 (2002).
7. N. Ben Abdallah, P. Degond, and P. A. Markowich, On a one-dimensional Schrödinger–Poisson scattering model, *Z. Angew. Math. Phys.* **48**, 135 (1997).
8. A. Bensoussan, J. L. Lions, and G. Papanicolaou, Boundary layers and homogenization of transport processes, *Publ. RIMS Kyoto Univ.* **15**, 53 (1979).
9. B. A. Biegel, *Simulation of Ultra-Small Electronic Devices: The Classical-Quantum Transition Region*, NASA Technical Report 97-028 (1997).
10. F. A. Buot and K. L. Jensen, Lattice Weyl–Wigner formulation of exact many-body quantum-transport theory and applications to novel solid-state quantum-based devices, *Phys. Rev. B* **42**, 9429 (1990).
11. S. Chandrasekhar, *Radiative Transfer* (Dover, New York, 1960).
12. Z. Chen, B. Cockburn, C. L. Gardner, and J. W. Jerome, Quantum hydrodynamic simulation of hysteresis in the resonant tunneling diode, *J. Comput. Phys.* **117**, 274 (1995).
13. F. Chevoir and B. Vinter, Scattering assisted tunneling in double-barrier diodes: Scattering rates and valley current, *Phys. Rev. B* **47**, 7260 (1993).
14. E. M. Conwell, High-field transport in semiconductor, in *Solid State Physics* (Academic Press, New York, 1967), Vol. g.
15. P. Degond and M. Lemou, On the viscosity and thermal conduction of fluids with multivalued internal energy, *Eur. J. Mech. B/Fluids* **20**, 303 (2001).

16. P. Degond and S. Mas-Gallic, Existence of solutions and diffusion approximation for a model Fokker–Planck equation, *Transp. Theor. Stat. Phys.* **16**, 589 (1987).
17. P. Degond and C. Schmeiser, Macroscopic models for semiconductor heterostructures, *J. Math. Phys.* **39**, 1 (1998).
18. A. El Ayyadi, *Couplage de Modles Classiques et Quantiques pour la Modlisation de Semiconducteurs*, Ph.D. thesis (Institut National des Sciences Appliques de Toulouse, in preparation).
19. B. C. Eu and K. Mao, Quantum kinetic theory of irreversible thermodynamics: Low-density gases, *Phys. Rev. E* **50**, 4380 (1994).
20. R. Ferreira and G. Bastard, Tunneling and relaxation in semiconductor double quantum wells, *Rep. Prog. Phys.* **60**, 345 (1997).
21. M. V. Fischetti, Theory of electron transport in small semiconductor devices using the Pauli Master equation, preprint (IBM Research Division, Yorktown Heights, New York).
22. W. R. Frensley, Boundary conditions for open quantum systems driven far from equilibrium, *Rev. Mod. Phys.* **62**, 745 (1990).
23. F. Golse, Knudsen layers from a computational viewpoint, *Transp. Theor. Stat. Phys.* **21**, 211 (1992).
24. F. Golse and A. Klar, A numerical method for computing asymptotic states and outgoing distributions for kinetic linear half-space problems, *J. Stat. Phys.* **80**(5–6), 1033 (1995).
25. F. Golse and F. Poupaud, Limite fluide des équations de Boltzmann des semiconducteurs pour une statistique de Fermi-Dirac, *Asymptotic Anal.* **6**, 135 (1992).
26. J. A. Kenrow, Quantum kinetic study of the electron-LO-phonon interaction in a semiconductor, *Phys. Rev. B* **55**, 7809 (1997).
27. N. C. Kluksdahl, A. M. Kriman, D. K. Ferry, and C. Ringhofer, Self-consistent study of the resonant-tunneling diode, *Phys. Rev. B* **39**, 7720 (1989).
28. W. Krech, A. Hädicke, and F. Seume, Master equation approach to macroscopic quantum tunneling of charge in ultrasmall single-electron-tunneling double junctions, *Phys. Rev. B* **48**, 5230 (1993).
29. E. W. Larsen and J. B. Keller, Asymptotic solution of neutron transport problems for small mean free paths, *J. Math. Phys.* **15**, 75 (1974).
30. I. B. Levinson, Translational invariance in uniform fields and the equation for the density matrix in the wigner representation, *Sov. Phys. JETP* **30**, 362 (1976).
31. R. K. Mains and G. I. Haddad, Wigner function modeling of resonant tunneling diodes with high peak to valley ratios, *J. Appl. Phys.* **64**, 5041 (1988).
32. R. K. Mains, J. P. Sun, and G. I. Haddad, Observation of intrinsic bistability in resonant tunneling diode modeling, *Appl. Phys. Lett.* **55**, 371 (1989).
33. P. Mounaix, O. Vanbésien, and D. Lippens, Effect of cathode spacer layer on the current voltage characteristics of resonant tunneling diodes, *Appl. Phys. Lett.* **57**, 1517 (1990).
34. R. Pinnau, The linearized transient quantum drift diffusion model—stability of stationary states, *ZAMMZ Angew. Math. Mech.* **80**, 327 (2000).
35. F. Poupaud, Diffusion approximation of the linear semicondictor Boltzmann equation analysis of boundary layers, *Asymptotic Anal.* **4**, 293 (1991).
36. W. H. Press, S. A. Teukolsky, W. T. Vetterling, and B. P. Flannery, *Numerical Recipes In Fortran 77*, Vol. 1, Cambridge University Press, Cambridge, UK, 1998.
37. E. Prugovecki, A quantum mechanical Boltzmann equation for one-particle Γ_s distribution functions, *Physica* **91 A**, 229 (1978).
38. L. Reggiani, Ed., *Hot-Electron Transport in Semiconductors* (Springer-Verlag, Berlin, 1985).
39. D. L. Rode, Low-field electron transport, in *Semiconductors and Semimetals* (Academic Press, New York, 1995), Vol. 10, p. 1.
40. S. M. Sze, *Physics of Semiconductor Devices* (Wiley, New York, 1969).
41. S. Selberherr, *Analysis and Simulation of Semiconductors* (Springer-Verlag, Berlin, 1984).
42. A. Yamnahakki, Second order boundary condition for the drift-diffusion equations of semiconductor, *Math. Models Meth. Appl. Sci.* **5**, 429 (1995).
43. T. Weil and B. Vinter, Calculation of phonon-assisted tunneling between two quantum wells, *J. Appl. Phys.* **60**, 3227 (1986).